© Goodwin, Graebe, Salgado , Prentice Hall 2000

Chapter 23

Model Predictive Control

© Goodwin, Graebe, Salgado , Prentice Hall 2000

Motivation

All real world control problems are subject to constraints of various types. The most common constraints are actuator constraints (amplitude and slew rate limits). In addition, many problems also have constraints on state variables (e.g. maximal pressures that cannot be exceeded, minimum tank levels, etc).

In many design problems, these constraints can be ignored, at least in the initial design phase. However, in other problems, these constraints are an inescapable part of the problem formulation since the system operates near a constraint boundary.

© Goodwin, Graebe, Salgado , Prentice Hall 2000

Motivation - *continued*

Chapter 11 described methods for dealing with constraints based on anti-windup strategies. These are probably perfectly adequate for simple problems - especially SISO problems. However, in more complex MIMO problems - especially those having both input and state constraints, it is frequently desirable to have a more formal mechanism for dealing with constraints in MIMO control system design.

© Goodwin, Graebe, Salgado , Prentice Hall 2000

Outline

We describe one such mechanism here based on Model Predictive Control. This has actually been a major success story in the application of modern control. More than 2,000 applications of this method have been reported in the literature - predominantly in the petrochemical area. Also, the method is being increasingly used in electromechanical control problems.

© Goodwin, Graebe, Salgado , Prentice Hall 2000

Advantages of Model Predictive Control

The main advantages of MPC are:

- it provides a one-stop-shop for MIMO control in the presence of constraints,
- it is one of the few methods that allows one to treat state constraints, and
- several commercial packages are available which give industrially robust versions of the algorithms aimed at chemical process control.

© Goodwin, Graebe, Salgado , Prentice Hall 2000

Anti-Windup Revisited

We assume that the complete state of a system is directly measured. Then, if one has a time-invariant model for a system and if the objectives and constraints are time-invariant, it follows that the control policy should be expressible as a fixed mapping from the state to the control. That is, the optimal control policy will be expressible as

$$u_x^o(t) = h(x(t))$$

for some static mapping $h(\circ)$. What remains is to give a characterization of the mapping $h(\circ)$.

© Goodwin, Graebe, Salgado , Prentice Hall 2000

We can think of the anti-windup strategies of Chapter 11 as giving a particular simple (ad-hoc) parameterization of *h*(∘). Specifically, if the control problem is formulated, in the absence of constraints, as a linear quadratic regulator, then we know that the unconstrained infinite horizon policy is of the form:

$$h^o(x(t)) = -K_\infty x(t)$$

© Goodwin, Graebe, Salgado , Prentice Hall 2000

State Space form of Anti-Windup

The anti-windup form of the above linear controller is

$$h(x(t)) = sat\{h^o(x(t))\}$$

where

$$h^o(x(t)) = -K_\infty x(t)$$

© Goodwin, Graebe, Salgado , Prentice Hall 2000

Example

We illustrate by a simple example.

Example 23.1: *Consider a continuous-time double integrator plant which is sampled with period Δ=1 second. The corresponding discrete time model is of the form*

$$
\begin{aligned}
x(k+1) &= \mathbf{A}x(k) + \mathbf{B}u(k) \\
y(k) &= \mathbf{C}x(k)
\end{aligned}
$$

where

$$
\mathbf{A} = \begin{bmatrix} 1 & 1 \\ 0 & 1 \end{bmatrix}; \qquad \mathbf{B} = \begin{bmatrix} 0.5 \\ 1 \end{bmatrix}; \qquad \mathbf{C} = \begin{bmatrix} 1 & 0 \end{bmatrix}
$$

© Goodwin, Graebe, Salgado , Prentice Hall 2000

We choose to use infinite horizon LQR theory to develop the control law. Within this framework, we use the following weighting matrices

$$\Psi = \mathbf{C}^T\mathbf{C}, \qquad \Phi = 0.1$$

We first consider the case when the control is unconstrained.

Then, for an initial condition of $x(0) = (-10, 0)^T$, the output response and input signal are as shown below.

© Goodwin, Graebe, Salgado , Prentice Hall 2000

Unconstrained Responses

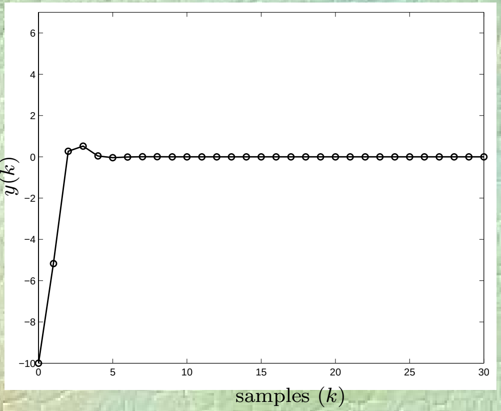

Figure 23.1:
Output response without constraints

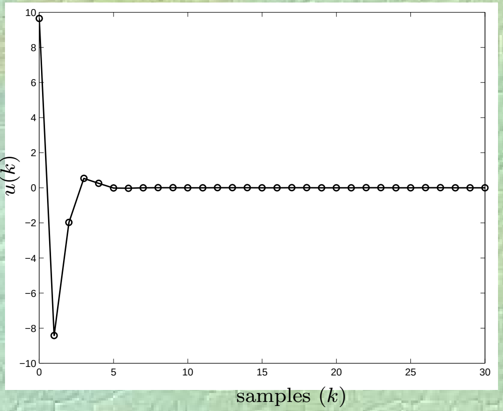

Figure 23.2:
Input response without constraints

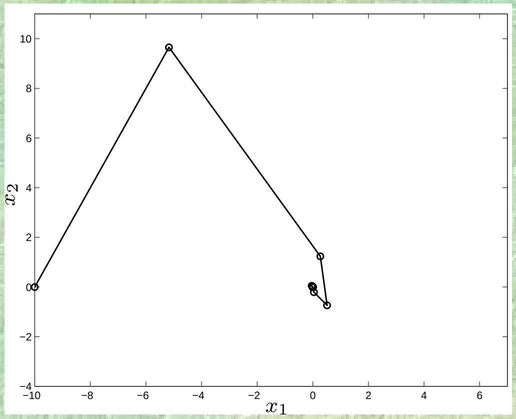

Figure 23.3:
Phase plane plot without constraints

© Goodwin, Graebe, Salgado , Prentice Hall 2000

Constraining the input amplitude

We next assume that the input must satisfy the mild constraint $|u(k)| \leq 5$. *Applying the anti-windup policy leads to the response shown on the next slide.*

© Goodwin, Graebe, Salgado , Prentice Hall 2000

Responses with Mild Constraint $|u(k)| \leq 5$

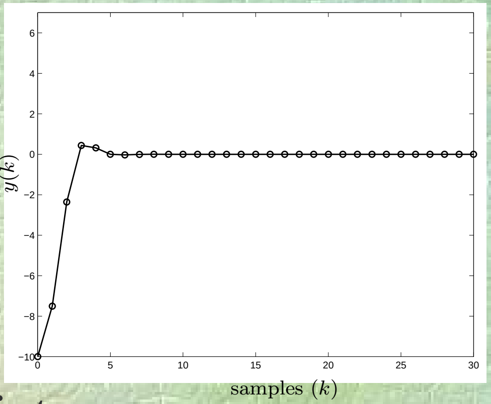

Figure 23.4: *Output response with input constraint* $|u(k)| \leq 5$

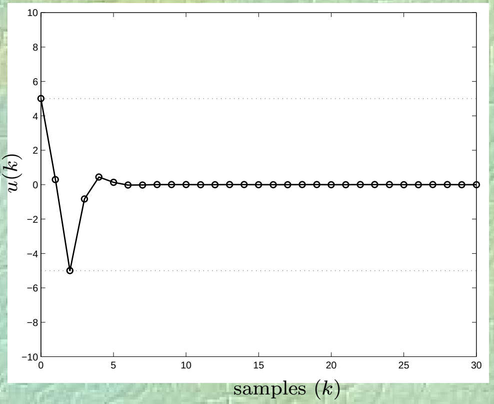

Figure 23.5: *Input response with constraint* $|u(k)| \leq 5$

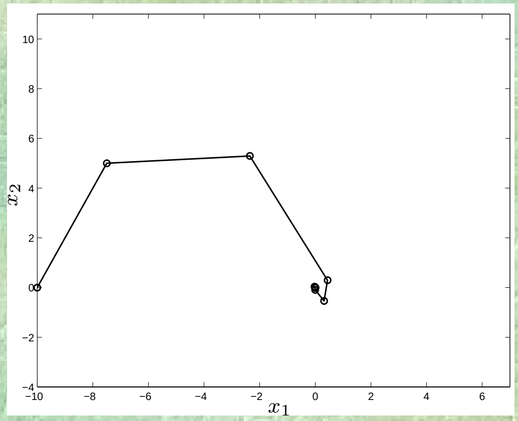

Figure 23.6: *Phase plane plot without constraint* $|u(k)| \leq 5$

© Goodwin, Graebe, Salgado , Prentice Hall 2000

Observations

The various plots indicate that the simple anti-windup strategy has produced a perfectly acceptable response in this case.

The above example would seem to indicate that one need never worry about fancy methods.

© Goodwin, Graebe, Salgado , Prentice Hall 2000

Making the constraint more severe

Example *Continued*. *Consider the same set up as above, save that the input is now required to satisfy the more severe constraint* $|u(k)| \leq 1$. *Notice that this constraint is 10% of the initial unconstrained input. Thus, this is a relatively severe constraint. The simple anti-windup control law now leads to the response shown on the next slide.*

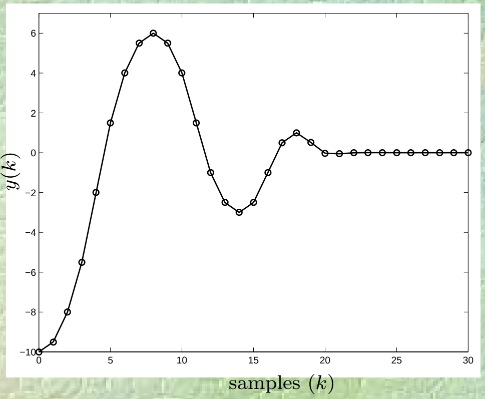

Figure 23.7:
Output response
with constraint |u(k)|≤ 1

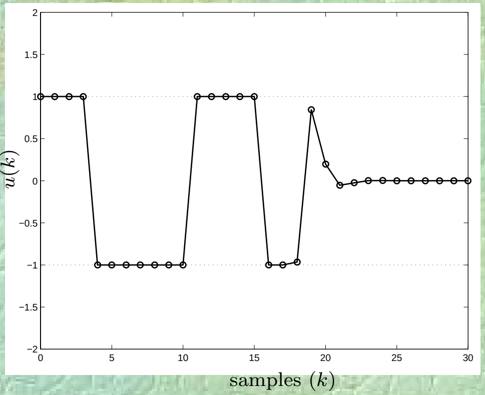

Figure 23.8:
Input response
with constraint |u(k)|≤ 1

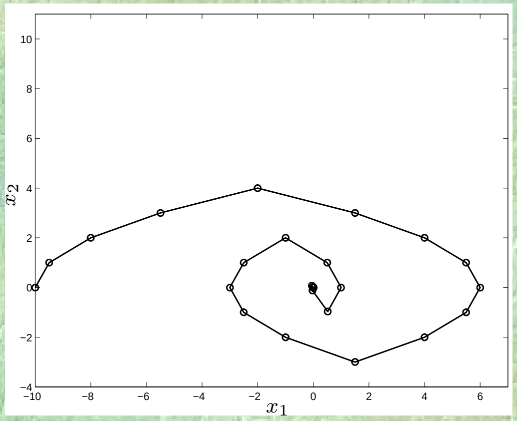

Figure 23.9:
Phase plane plot
with constraint |u(k)|≤ 1

© Goodwin, Graebe, Salgado , Prentice Hall 2000

Observations

We see that the simple anti-windup strategy is not performing well and, indeed, has resulted in large overshoot in this case.

© Goodwin, Graebe, Salgado , Prentice Hall 2000

Discussion of Example with Severe Constraints

We see that the initial input steps have caused the velocity to build up to a large value. If the control were unconstrained, this large velocity would help us get to the origin quickly. However, because of the limited control authority, the system *braking capacity* is restricted and hence large overshoot occurs. In conclusion, it seems that the control policy has been too *shortsighted* and has not been able to account for the fact that future control inputs would be constrained as well as the current control input. The solution would seem to be to try to *look-ahead* (i.e. predict the future response) and to take account of *current* and *future* constraints in deriving the control policy. This leads us to the idea of model predictive control.

© Goodwin, Graebe, Salgado , Prentice Hall 2000

What is Model Predictive Control?

Model Predictive Control is a control algorithm based on solving an on-line optimal control problem. A *receding horizon* approach is used which can be summarized in the following steps:

(*i*) At time k and for the current state $x(k)$, solve, on-line, an open-loop optimal control problem over some future interval taking account of the current and *future* constraints.

(*ii*) Apply the first step in the optimal control sequence.

(*iii*) Repeat the procedure at time $(k+1)$ using the current state $x(k+1)$.

© Goodwin, Graebe, Salgado , Prentice Hall 2000

Turning the solution into a closed loop policy

The solution is converted into a closed loop strategy by using the measured value of $x(k)$ as the current state. When $x(k)$ is not directly measured then one can obtain a closed loop policy by replacing $x(k)$ by an estimate provided by some form of observer.

© Goodwin, Graebe, Salgado , Prentice Hall 2000

Details for Nonlinear Model

Given a model

$$x(\ell+1) = f(x(\ell), u(\ell)), \qquad x(k) = x$$

the MPC at event (*x*, *k*) is computed by solving a constrained optimal control problem:

$$\mathcal{P}_N(x): \qquad V_N^o(x) = \min_{U \in \mathcal{U}_N} V_N(x, U)$$

where

$$U = \{u(k), u(k+1), \dots, u(k+N-1)\}$$

$$V_N(x, U) = \sum_{\ell=k}^{k+N-1} L(x(\ell), u(\ell)) + F(x(k+N))$$

and $\mathcal{U}_N$ is the set of *U* that satisfy the constraints over the entire interval [*k*, *k* + *N* - 1]; i.e.

© Goodwin, Graebe, Salgado , Prentice Hall 2000

$$\begin{aligned} u(\ell) &\in \mathbb{U} \qquad & \ell &= k, k+1, \ldots, k+N-1 \\ x(\ell) &\in \mathbb{X} \qquad & \ell &= k, k+1, \ldots, k+N \end{aligned}$$

together with the terminal constraint

$$x(k+N) \in W$$

Usually $\mathsf{U} \subset \mathsf{R}^m$ is convex and compact, $\mathsf{X} \subset \mathsf{R}^n$ is convex and closed, and W is a set that can be appropriately selected to achieve stability.

In the above formulation, the model and cost function are time invariant. Hence, one obtains a time-invariant feedback control law.

$$\mathcal{P}_N(x): \qquad V_N^o(x) = \min_{U \in \mathcal{U}_N} V_N(x, U)$$

$$U = \{u(0), u(1), \ldots, u(N-1)\}$$

$$V_N(x, U) = \sum_{\ell=0}^{N-1} L(x(\ell), u(\ell)) + F(x(N))$$

$$U_x^o = \{u_x^o(0), u_x^o(1), \ldots, u_x^o(N-1)\}$$

Then, the actual control applied at time k is the first element of this sequence, i.e.

$$u = u_x^o(0)$$

Figure 23.10: *Receding horizon control principle*

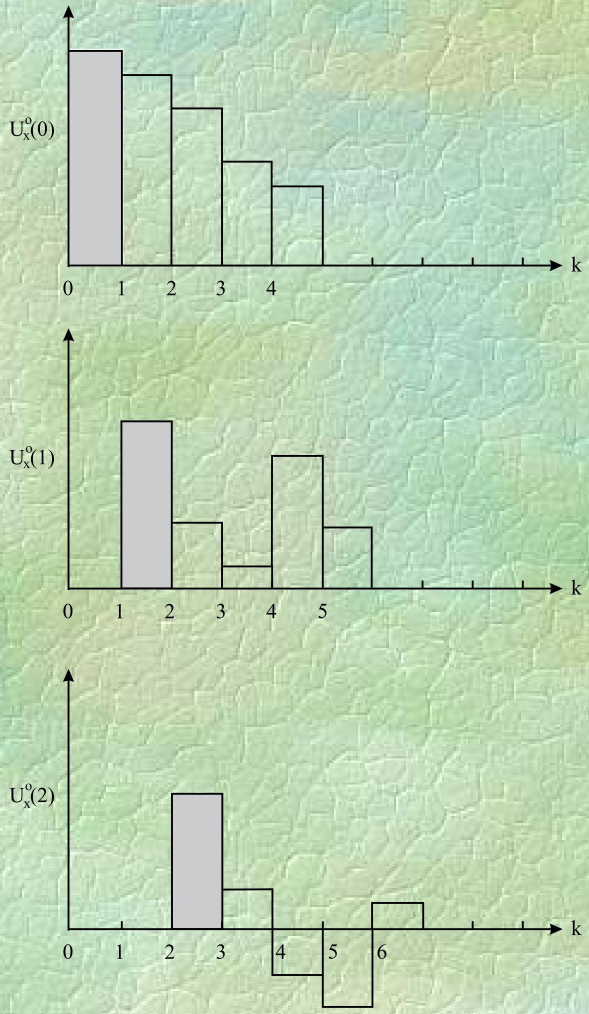

© Goodwin, Graebe, Salgado , Prentice Hall 2000

An alternative view of Receding Horizon optimization is shown on the next slide

© Goodwin, Graebe, Salgado , Prentice Hall 2000

Alternative View of Receding Horizon Control Policy

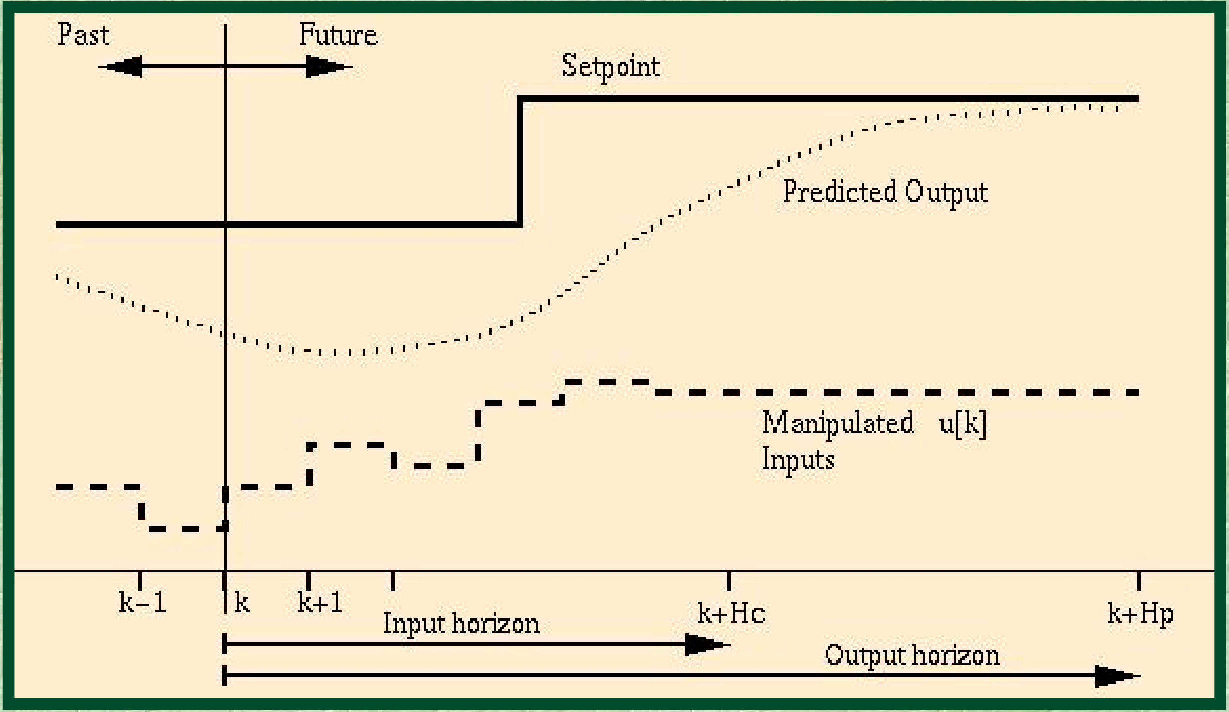

© Goodwin, Graebe, Salgado , Prentice Hall 2000

The associated literature can be divided into four generations as follows:

- *First generation* (1970's) - used impulse or step response linear models, quadratic cost function, and ad-hoc treatment of constraints.
- *Second generation* (1980's) - linear state space models, quadratic cost function, input and output constraints expressed as linear inequalities, and quadratic programming used to solve the constrained optimal control problem.
- *Third generation* (1990's) - several levels of constraints (soft, hard, ranked), mechanisms to recover from infeasible solutions.
- *Fourth generation* (late 1990's) - nonlinear problems, guaranteed stability, and robust modifications.

© Goodwin, Graebe, Salgado , Prentice Hall 2000

Stability

A remarkable property of MPC is that one can establish stability of the resultant feedback system (at least with full state information). This is made possible by the fact that the value function of the optimal control problem acts as a Lyapunov function for the closed loop system.

© Goodwin, Graebe, Salgado , Prentice Hall 2000

Assumptions

For clarity of exposition, we make the following simplifying assumptions:

A1: An additional constraint is placed on the final state

$$x(N) = 0$$

A2: $L(x, u)$ is positive definite in both arguments.

© Goodwin, Graebe, Salgado , Prentice Hall 2000

Theorem 23.1: *Consider the system controlled by the receding horizon MPC algorithm and subject to a terminal constraint. This control law renders the resultant closed loop system globally asymptotically stable.*

© Goodwin, Graebe, Salgado , Prentice Hall 2000

Details of Proof

The value function $V_N^0(\cdot)$ is positive definite and proper ($V(x) \to \infty$ as $||x|| \to \infty$). It can therefore be used as a Lyapunov function for the problem. We recall that at event (x, k), MPC solves:

$$\mathcal{P}_N(x): \qquad V_N^o(x) = \min_{U \in \mathcal{U}_N} V_N(x, U)$$

$$V_N(x, U) = \sum_{\ell=0}^{N-1} L(x(\ell), u(\ell)) + F(x(N))$$

subject to constraints.

© Goodwin, Graebe, Salgado , Prentice Hall 2000

Proof continued:

We denote the optimal open loop control sequence solving $\mathsf{P}_N(x)$ as

$$U_x^o = \{u_x^o(0), u_x^o(1), \ldots, u_x^o(N-1)\}$$

We recall that inherent in the MPC strategy is the fact that the actual control applied at time *k* is the first value of this sequence; i.e.

$$u = h(x) = u_x^o(0)$$

Let $x(1) = f(x, h(x))$ and let $x(N)$ be the terminal state resulting from the application of U_x^0. Note that we are assuming $x(N) = 0$.

© Goodwin, Graebe, Salgado , Prentice Hall 2000

Proof continued:

A feasible solution (but not the optimal one) for the second step in the receding horizon computation $\mathsf{P}_N(x_1)$ is then:

$$\tilde{U}_x = \{u_x^o(1), u_x^o(2), \dots, u_x^o(N-1), 0\}$$

Then the increment of the Lyapunov function on using the true MPC optimal input and when moving from *x* to *x*(1) = *f*(*x*, *h*(*x*)) satisfies:

$$\begin{aligned}\Delta_h V_N^o(x) &\triangleq V_N^o(x(1)) - V_N^o(x)\\ &= V_N(x(1), U_{x_1}^o) - V_N(x, U_x^o)\end{aligned}$$

© Goodwin, Graebe, Salgado , Prentice Hall 2000

Proof continued:

However, since $U_{x_1}^0$ is optimal, we know that

$$V_N(x(1), U_{x_1}^o) \leq V_N(x(1), \tilde{U}_x)$$

where $\tilde{U}_x$ is the sub-optimal sequence defined earlier. Hence, we have

$$\Delta_h V_N^o(x) \leq V_N(x(1), \tilde{U}_x) - V_N(x, U_x^o)$$

Proof continued:

Using the fact that $\tilde{U}_x$ shares (N-1) terms in common with U_x^0, we can see that the right hand side satisfies:

$$V_N(x(1), \tilde{U}_x) - V_N(x, U_x^o) = -L(x, h(x))$$

where we have used the fact that U_x^0 leads to $x(N) = 0$ by assumption and hence $\tilde{U}_x$ leads to $x(N+1) = 0$.

Finally we have

$$\Delta_h V_N^o(x) \leq -L(x, h(x))$$

When $L(x, u)$ is positive definite in both arguments, then stability follows immediately from the Lyapunov Stability Theorem.

© Goodwin, Graebe, Salgado , Prentice Hall 2000

Beyond the issue of stability, a user of MPC would clearly also be interested in what, if any performance advantages are associated with the use of this algorithm. In an effort to (partially) answer this question, we pause to revisit the earlier example.

© Goodwin, Graebe, Salgado , Prentice Hall 2000

Example Revisited

Consider again the problem described earlier with input constraint $|u(k)| \leq 1$. We recall that the *shortsighted* policy led to large overshoot.

Here, we consider the MPC cost function with $N = 2$ and such that $F(x(N))$ is the optimal *unconstrained* infinite horizon cost and $L(x(\ell), u(\ell))$ is the incremental cost associated with the underlying LQR problem.

Here we consider the constraint on the present and next step. Thus the derivation of the control policy is not quite as *shortsighted* as was previously the case.

Results for MPC with constraints applied on first two steps

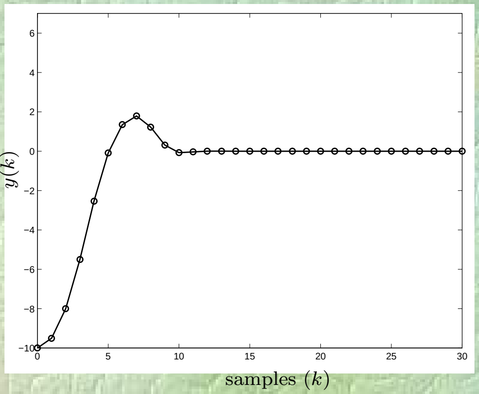

Figure 23.11: *Output response using MPC*

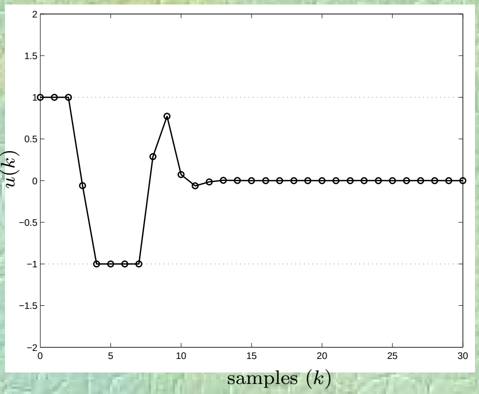

Figure 23.12: *Input response using MPC*

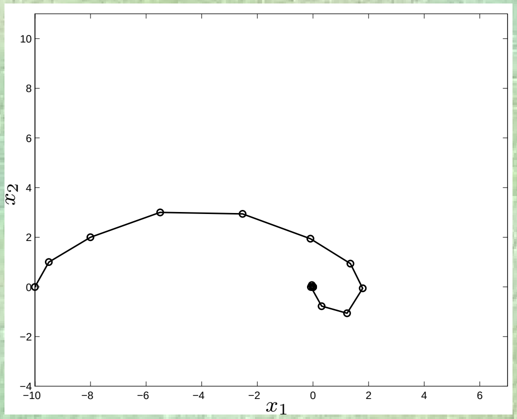

Figure 23.13: *Phase plane plot using MPC*

© Goodwin, Graebe, Salgado , Prentice Hall 2000

Observations

Comparing these results with those obtained earlier, we see that the performance has been significantly improved. This is because the policy is no longer quite so shortsighted as it previously was. Thus we see that MPC can indeed over performance advantages over the shortsighted anti-windup strategy

© Goodwin, Graebe, Salgado , Prentice Hall 2000

Linear Models with Quadratic Cost Function

Model:
$$x(\ell+1) = \mathbf{A}x(\ell) + \mathbf{B}u(\ell)$$
$$y(\ell) = \mathbf{C}x(\ell)$$

Error:
$$e(\ell) = y(\ell) + (d(\ell) - y_s)$$

Combined "disturbance":
$$d_e(\ell) = d(\ell) - y_s$$

Cost:
$$\begin{aligned} J_o =& [x(N) - x_s]^T \boldsymbol{\Psi}_f [x(N) - x_s] \\ &+ \sum_{\ell=0}^{N-1} e^T(\ell)\boldsymbol{\Psi} e(\ell) \\ &+ \sum_{\ell=0}^{M-1} [u(\ell) - u_s]^T \boldsymbol{\Phi} [u(\ell) - u_s] \end{aligned}$$

© Goodwin, Graebe, Salgado , Prentice Hall 2000

It can be shown that, if the design is unconstrained, J_0 is minimized by taking

$$U = -\mathbf{W}^{-1}\mathbf{V}$$

where **W** and **V** are functions of **A**, **B**, **C** matrices. **V** is also a function of the disturbances and desired output.

Magnitude and rate constraints on both the plant *input* and *output* can be easily expressed as *linear* constraints on U of the form

$$LU \le K$$

© Goodwin, Graebe, Salgado , Prentice Hall 2000

QP Solution

Thus the constrained problem takes the form:

$$U^{OPT} = \arg \min_{\substack{U \\ LU \leq K}} U^T \mathbf{W} U + 2U^T \mathbf{V}$$

This optimization is a convex problem due to the quadratic cost and linear constraints. Also, standard numerical procedures (called Quadratic Programming algorithms or QP for short) are available to solve this sub-problem.

© Goodwin, Graebe, Salgado , Prentice Hall 2000

Summary of Key Idea

- Solve receding horizontal optimal control problem subject to constraints

$$V = \underset{\substack{u\in U\\ x\in\Omega}}{Min}\; x_N^T P_N x_N + \sum_{k+1}^{N} x_k^T Q x_k + u_k^T R u_k$$

- Apply first step of control - move forward one step

- Stability can be established - terminal constraint of *x* crucial.

Example

Plant: $G(s) = \dfrac{3}{s^2 + 0.2s + 1}$

Desired Output: $Y_{ss} = 1$

Steady State Input: $U_{ss} = 0.33$

Constraint on Input: $|u| < 0.4$

© Goodwin, Graebe, Salgado , Prentice Hall 2000

Results: *dashed line - unconstrained input*
solid line - constrained input found via MPC

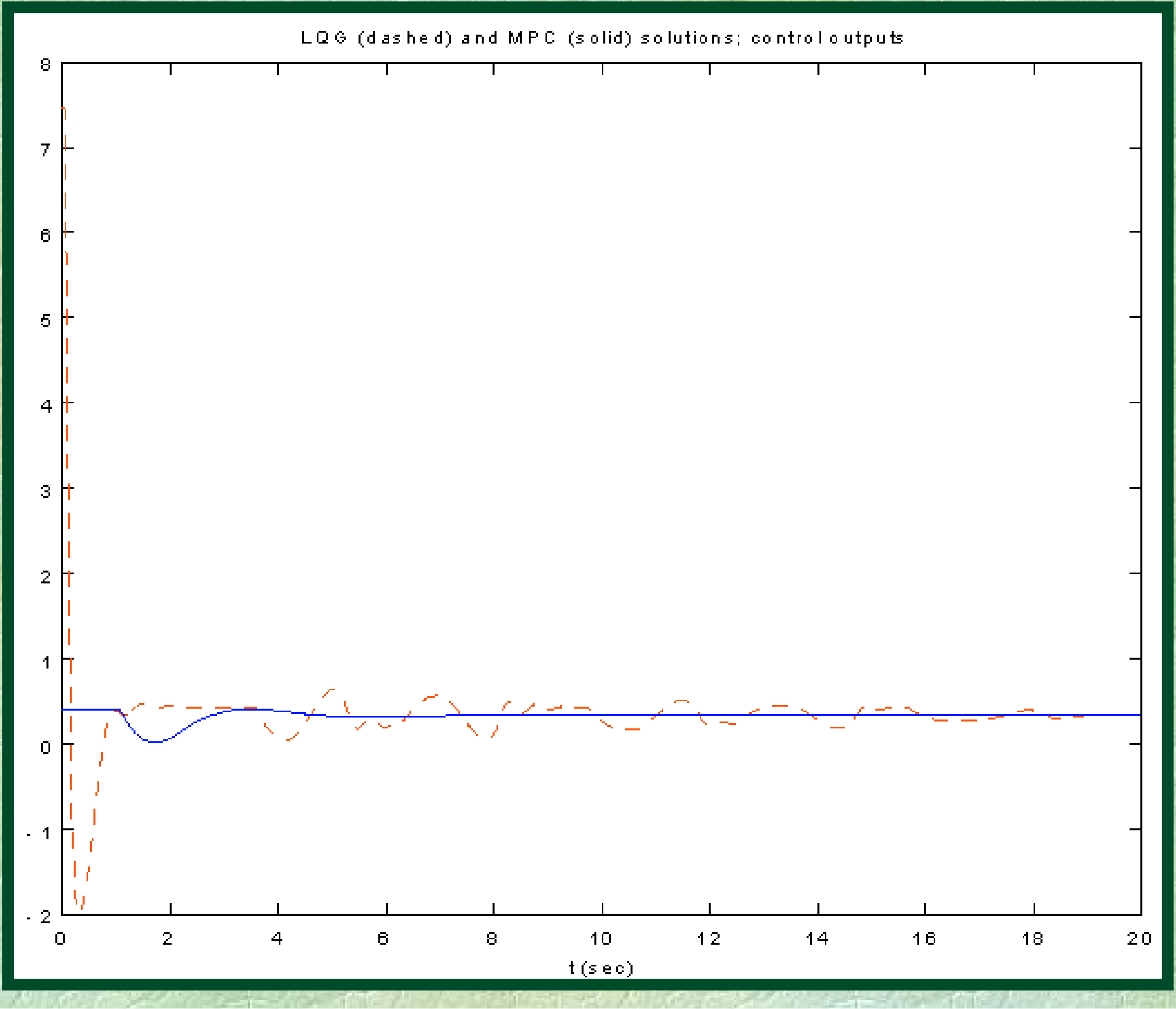

© Goodwin, Graebe, Salgado , Prentice Hall 2000

Output Response: Dashed line - *response when unconstrained input is saturated and applied to plant*

Solid line - *response obtained from MPC algorithm*

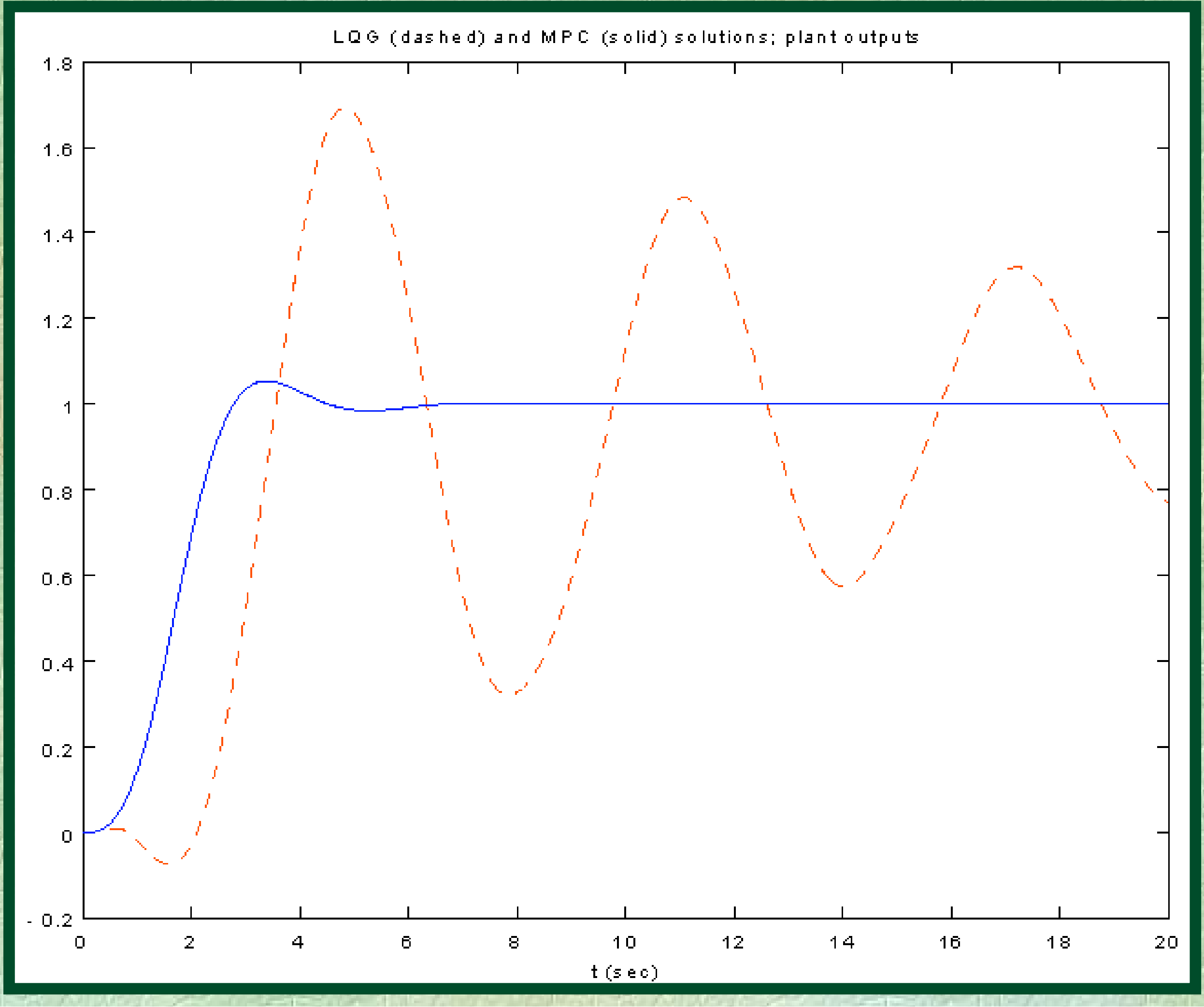

© Goodwin, Graebe, Salgado , Prentice Hall 2000

One Degree of Freedom Controller

A one-degree of freedom output feedback controller is obtained by including the set point in the quantities to be estimated. The resultant output feedback MPC strategy is schematically depicted below.

© Goodwin, Graebe, Salgado , Prentice Hall 2000

Figure 23.14: *One-degree-of-freedom MPC architecture*

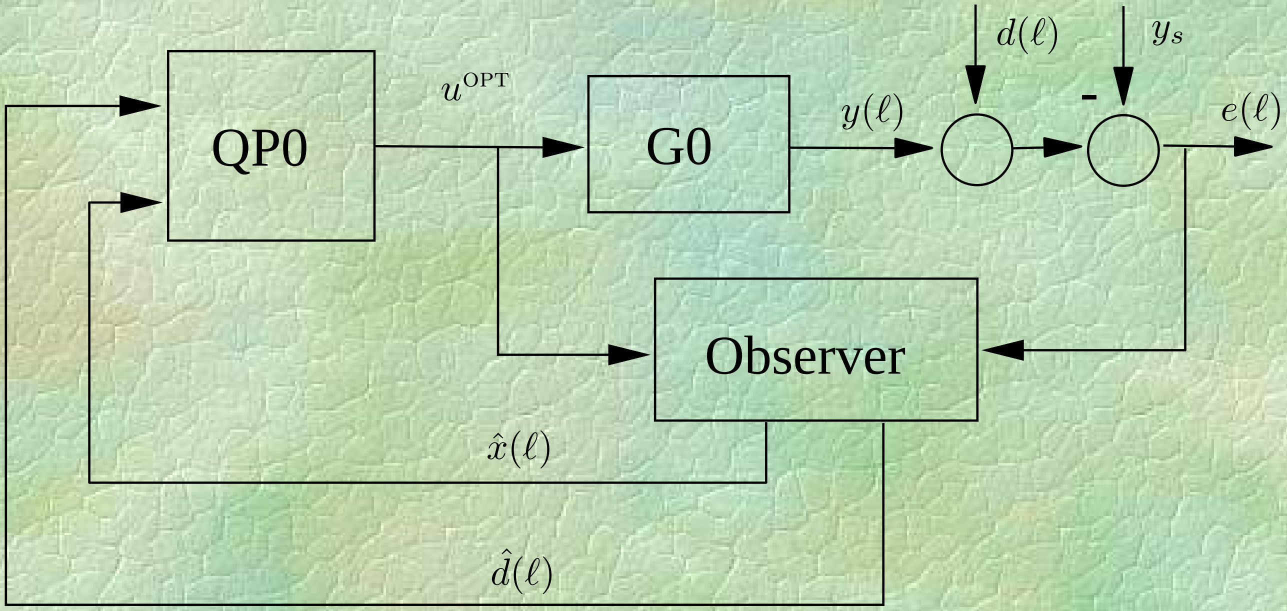

© Goodwin, Graebe, Salgado , Prentice Hall 2000

Integral Action

An important observation is that the architecture described above gives a form of integral action. In particular y is taken to the set-point y_s irrespective of the true plant description (provided a steady state is reached and provided that, in this steady state, u is not constrained).

© Goodwin, Graebe, Salgado , Prentice Hall 2000

Rudder Roll Stabilization of Ships

Here we present a realistic application of model predictive control to rudder roll stabilization of ships.

It is desirable to reduce the rolling motion of ships produced by wave action so as to prevent cargo damage and improve crew efficiency and passenger comfort. Conventional methods for ship roll stabilization include water tanks, stabilization fins and bilge keels. Another alternative is to use the rudder for roll stabilization as well as course keeping. However, using the rudder for simultaneous course keeping and roll reduction is non-trivial since only one actuator is available to deal with two objectives.

Constraint

An important issue in this problem is that the rudder mechanism is usually limited in amplitude and slew rate. Hence this is a suitable problem for model predictive control.

© Goodwin, Graebe, Salgado , Prentice Hall 2000

Figure 23.15: *Magnitudes and conventions for ship motion description*

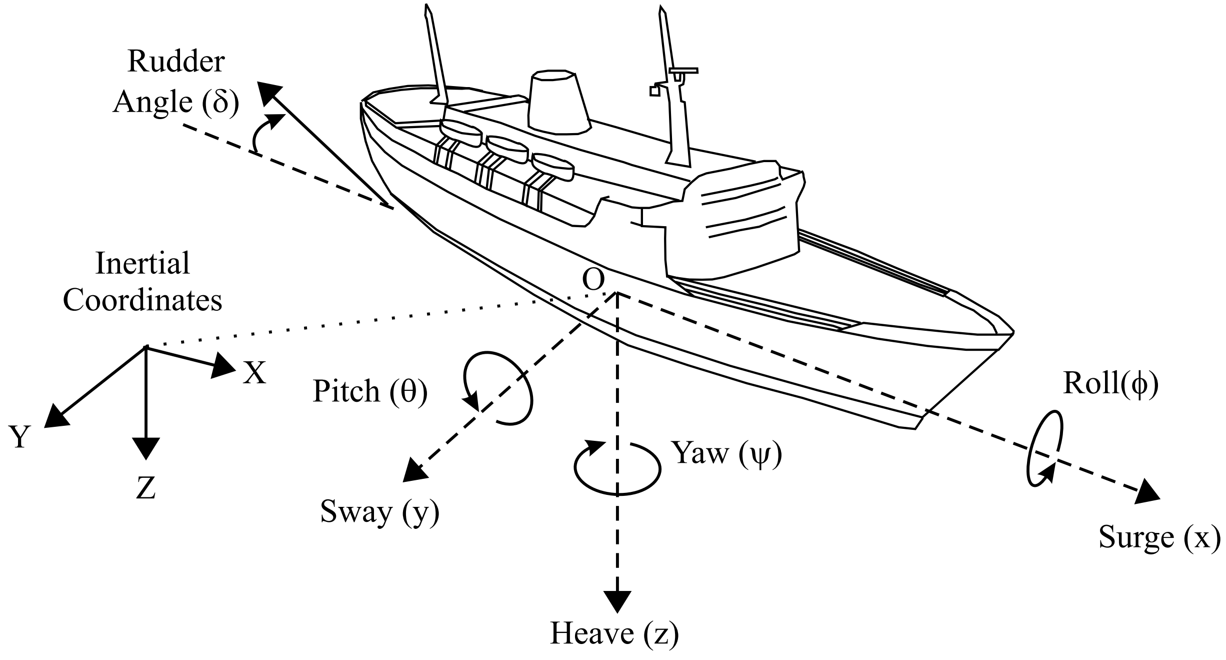

The Model

Wave disturbances are usually considered at the output, and the complete model of the ship dynamics including the output equation is of the form:

$$\dot{x} = \mathbf{A}x + \mathbf{B}\delta$$
$$y = \mathbf{C}x + d_{wave}$$

where only the roll and yaw are typically directly measured i.e. $y := [\ \ ,\ \ ]^{\mathrm{T}}$. d_{wave} is the wave induced disturbance on the output variables.

© Goodwin, Graebe, Salgado , Prentice Hall 2000

Model for Wave Disturbances

The wave disturbances can be characterized in terms of their frequency spectrum. This frequency spectrum can be simulated by using filtered white noise. The filter used to approximate the spectrum is usually a second order one of the form

$$H(s) = \frac{K_w s}{s^2 + 2\xi\omega_0 s + \omega_0^2}$$

© Goodwin, Graebe, Salgado , Prentice Hall 2000

Control Objectives

The design objectives for rudder roll stabilization are:

- Increase the damping and reduce the roll amplitude
- Control the heading of the ship

© Goodwin, Graebe, Salgado , Prentice Hall 2000

Details of the Model

The following model was used for the ship

$$\mathbf{A} = \begin{bmatrix} -0.1795 & -0.8404 & 0.2115 & 0.9665 & 0 \\ -0.0159 & -0.4492 & 0.0053 & 0.0151 & 0 \\ 0.0354 & -1.5594 & -0.1714 & -0.7883 & 0 \\ 0 & 0 & 1 & 0 & 0 \\ 0 & 1 & 0 & 0 & 0 \end{bmatrix}$$

$$\mathbf{B} = \begin{bmatrix} 0.2784 \\ -0.0334 \\ -0.0894 \\ 0 \\ 0 \end{bmatrix}$$

This system was sampled with a zero order hold and sampling period of 0.5.

© Goodwin, Graebe, Salgado , Prentice Hall 2000

Details of the Optimization Criterion

Details of the model predictive control optimization criterion were that a standard LQR cost function was employed with

$$\Psi = \begin{bmatrix} 90 & 0 \\ 0 & 3 \end{bmatrix}; \qquad \Phi = 0.1$$

Optimization horizon, $N = 20$; Control horizon $M = 18$.

© Goodwin, Graebe, Salgado , Prentice Hall 2000

Estimating the System State

Since only roll, , and yaw, , were assumed to be directly measured, then a Kalman filter was employed to estimate the 5 system states and 2 noise states in the composite model.

The results of applying MPC to this problem are shown on the following slides.

We consider three cases:

(*i*) No constraints on the rudder

(*ii*) Rudder constrained to a maximum angle of 30 degrees and a maximum slew rate of 15 degrees per second

(*iii*) Rudder constrained to a maximum angle of 20 degrees and a maximum slew rate of 8 degrees per second.

© Goodwin, Graebe, Salgado , Prentice Hall 2000

Figure 23.16: *Ship motion with no constraints on rudder motion*

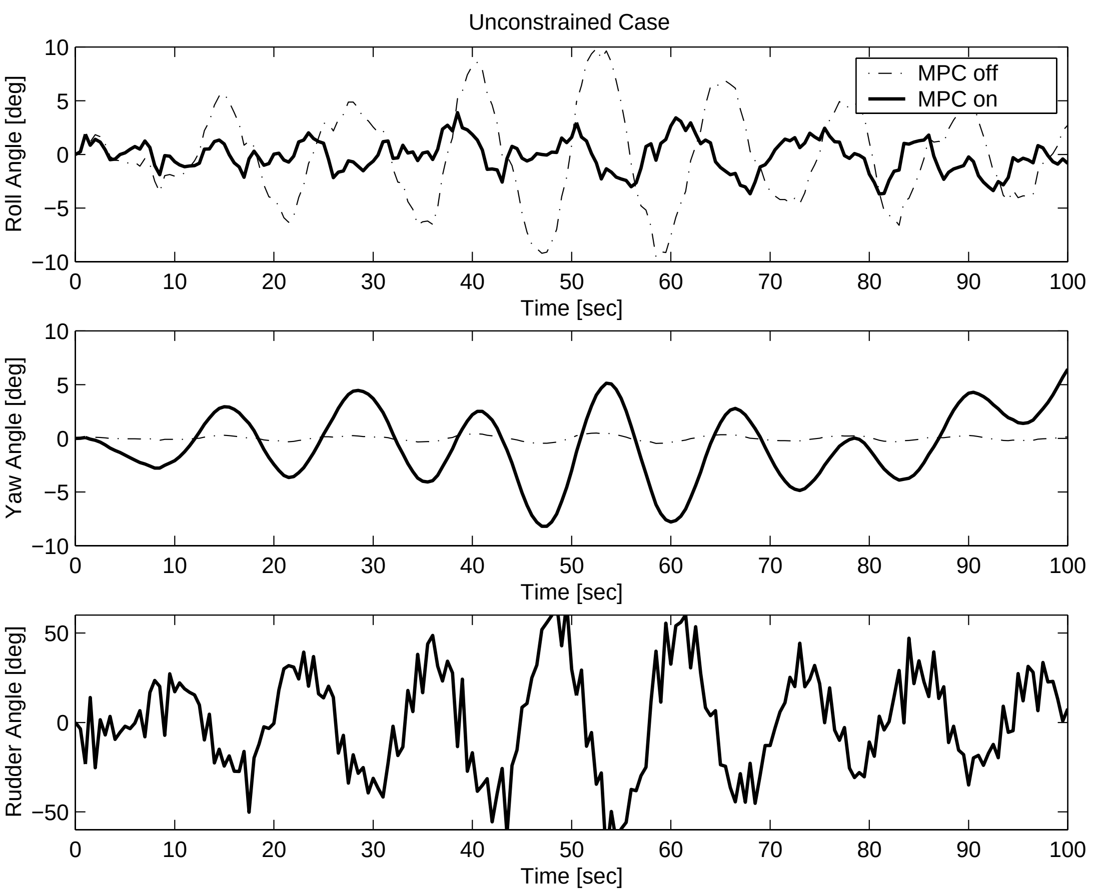

© Goodwin, Graebe, Salgado , Prentice Hall 2000

Figure 23.17: *Ship motion when rudder constrained to maximum angle of 30 degrees and maximum slew rate of 15 degrees/sec.*

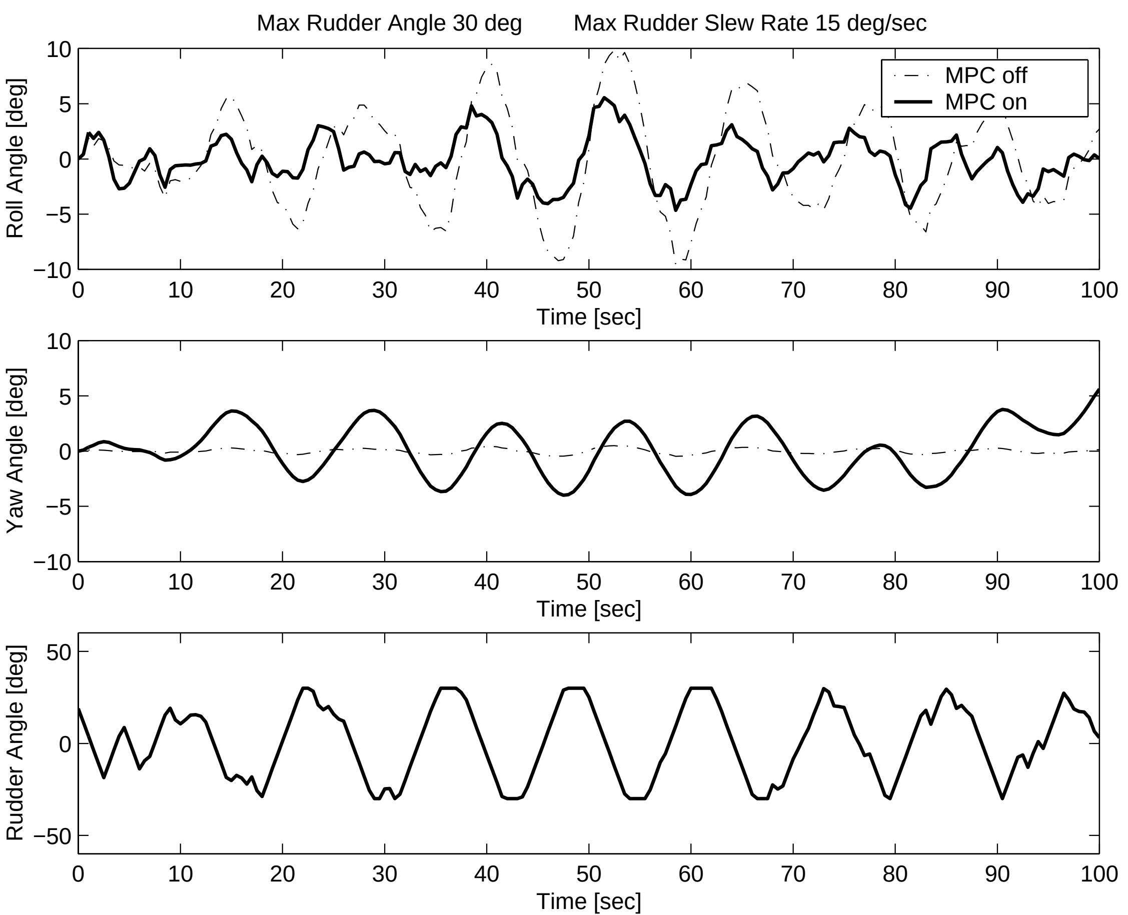

© Goodwin, Graebe, Salgado , Prentice Hall 2000

Figure 23.18: *Ship motion when rudder constrained to maximum angle of 20 degrees and maximum slew rate of 8 degrees/sec.*

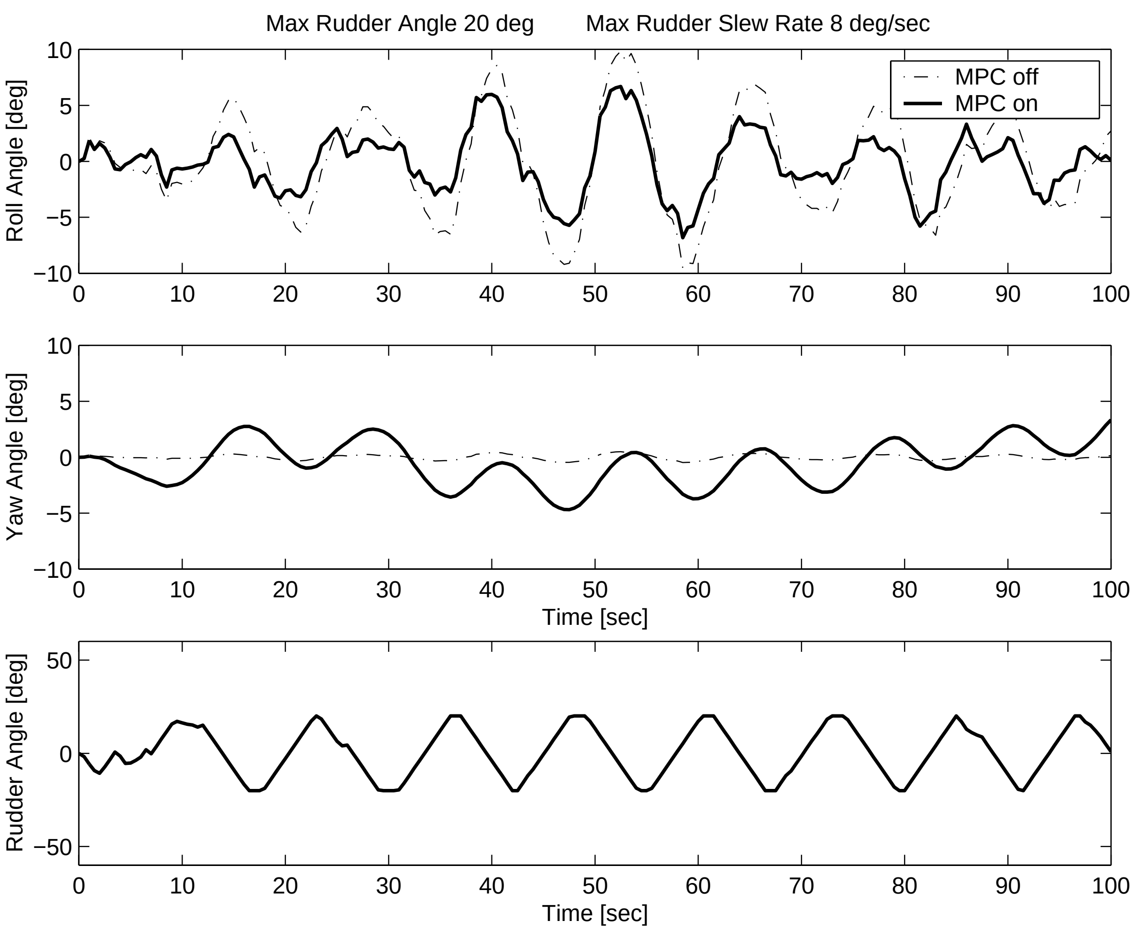

© Goodwin, Graebe, Salgado , Prentice Hall 2000

Observations

We see that MPC offers a satisfactory solution to this problem. Roll motion has been significantly reduced and, when reformulated as part of the problem description, constraints on maximum rudder angle and slew rate have been imposed.

© Goodwin, Graebe, Salgado , Prentice Hall 2000

Another Example:

Fluid Catalytic Reactor Modeling and Control using MPC

This section contributed by:
Jia Chunyang, S. Rohani and Arthur Jutan
Dept. of Chemical & Biochemical Engineering
The University of Western Ontario
London, Ontario, Canada

© Goodwin, Graebe, Salgado , Prentice Hall 2000

FCC Unit Modeling and MPC Control Simulation

The profitability of a Fluidized Catalyst Cracking Unit makes it of supreme importance in an oil refinery.

A typical FCC process diagram is shown in Figure 1.

Model Development

- A.Malay and S.Rohani have developed a reliable and simple model in 1998. They used a four lump kinetic scheme. See Fig. 2
- The model involves 40 algebraic and ordinary differential equations.

© Goodwin, Graebe, Salgado , Prentice Hall 2000

Figure 1: *FCC Unit Process and Control Diagram*

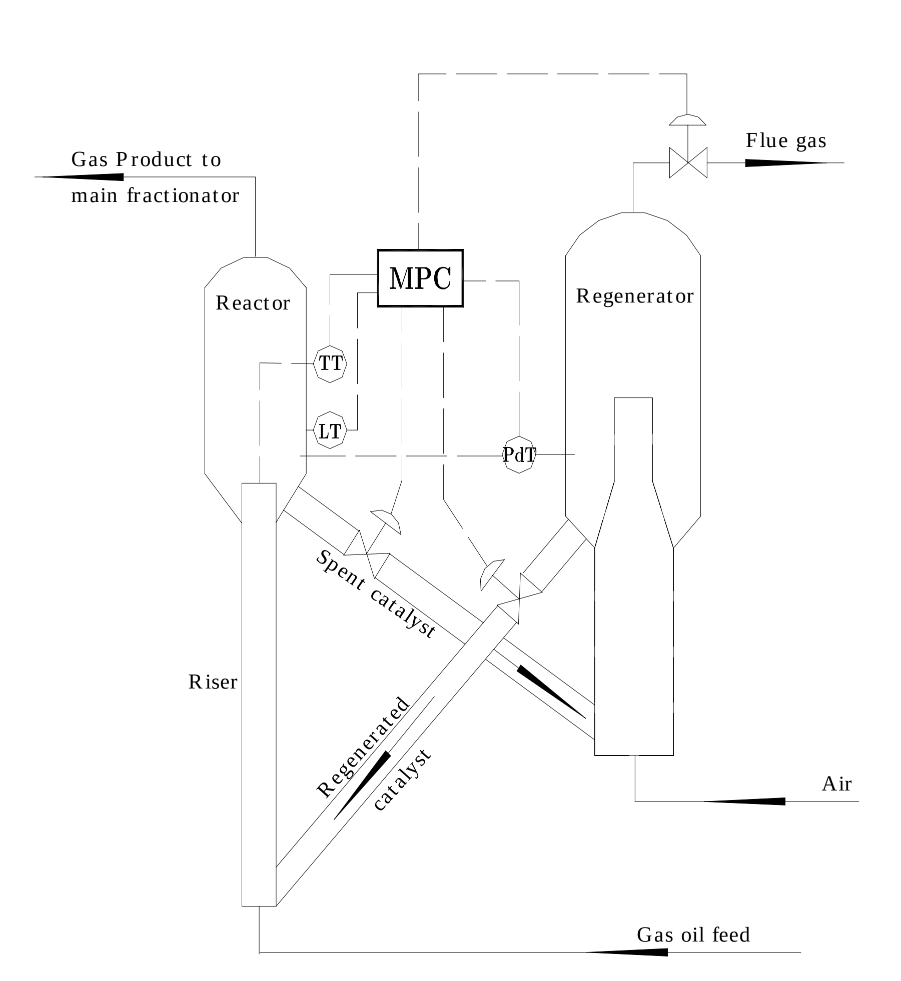

© Goodwin, Graebe, Salgado , Prentice Hall 2000

The variables are:

- Controlled variables (*CVs*):
  - Riser outlet temperature (T_{ris})
  - Reactor bed and regenerator differential pressure (*Pd*)
  - Reactor bed level (L_{rct})
- Manipulated variables (*MVs*):
  - Regenerated catalyst flow rate (V_{reg})
  - Flue gas flow rate (V_{flu})
  - Spent catalyst flow rate (V_{spt})

© Goodwin, Graebe, Salgado , Prentice Hall 2000

- Disturbances (*DVs*):
  - Gas oil feed flow rate (F_{gas})
  - Air flow rate (F_{air})

Figure 2: *Four lump kinetic scheme*

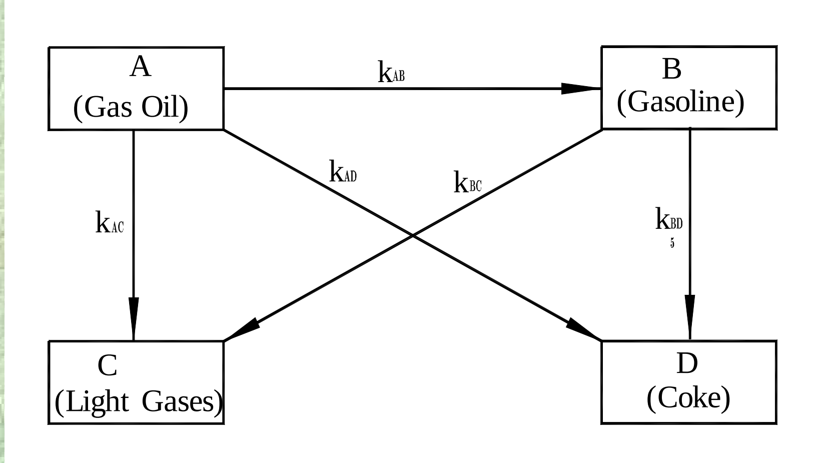

Model predictive control simulation

The principle of MPC maybe expressed in the following way: Based on a model of the process, predictive control is the control strategy that makes the predicted process dynamic output equal to a desired dynamic output conveniently predefined.

The quadratic objective of the MPC control strategy:

$$\min \quad \sum_{l=1}^{\mathrm{p}} \left\| \Gamma_l^y \left[y(k+l|k) - r(k+l) \right] \right\|^2 + \sum_{l=1}^{m} \left\| \Gamma_l^u \left[\Delta u(k+l-1) \right] \right\|^2$$

$$\Delta u(k) \cdots \Delta u(k+m-1)$$

© Goodwin, Graebe, Salgado , Prentice Hall 2000

Control problem formulation

The open loop system is modeled as follows:

$$y = Gu + G_d d$$

where, $u=[V_{reg} \quad V_{flu} \quad V_{spt}]^T$,

$y=[T_{ris} \quad Pd \quad L_{rct}]^T$,

$d=[F_{gas} \quad F_{air}]^T$,

G is the plant model and G_d is the disturbance model.

© Goodwin, Graebe, Salgado , Prentice Hall 2000

Offline model identification

- Data acquisition

  In order to acquire the process data which contain sufficient information, we must carefully design a step test in terms of the input amplitude and frequency.

- Offline identification

  The process data must be handled carefully. This work has mainly been done through state space N4SID method and trial and error.

  The impulse response of the system can be obtained:

$$\hat{g}(\tau) = \frac{1}{\lambda N} \sum_{t=1}^{N} y(t+\tau)u(t)$$

Then the system transfer function G(z) can be obtained:

$$G(z) = \sum_{k=1}^{\infty} g(k) z^{-k}$$

© Goodwin, Graebe, Salgado , Prentice Hall 2000

Open loop dynamic responses

Open loop dynamic responses, see Figures 3-5, show highly nonlinear and strong coupling characteristics of the process.

© Goodwin, Graebe, Salgado , Prentice Hall 2000

Figure 3: *Transient response of the system for input changes in the regenerated catalyst valve opening. (10% step increase at 0.5 hrs, 20% step decrease at 4 hrs, 10% increase at 8 hrs).*

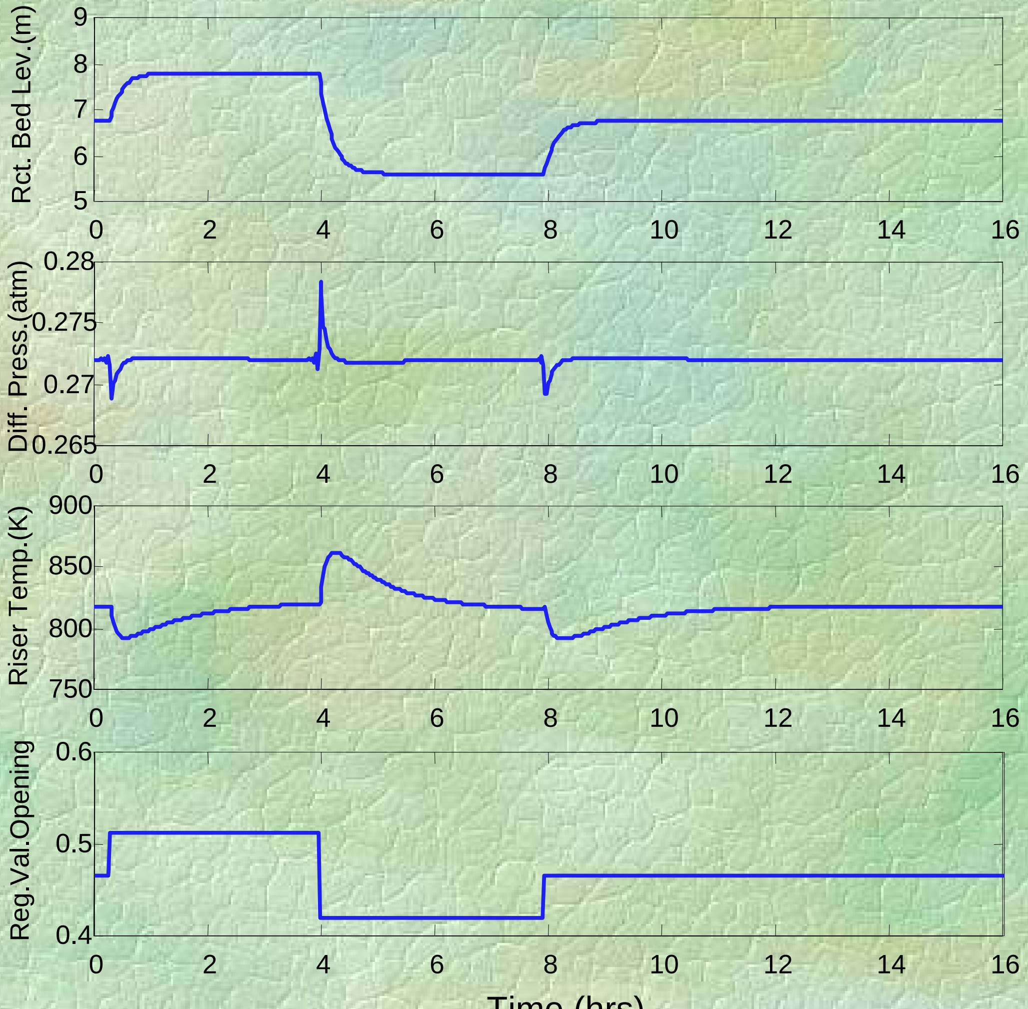

© Goodwin, Graebe, Salgado , Prentice Hall 2000

Figure 4: *Transient response of the system for input changes in the flue gas valve opening. (4% step increase at 0.5 hrs, 7% step decrease at 5.2 hrs, 3% increase at 10.5 hrs).*

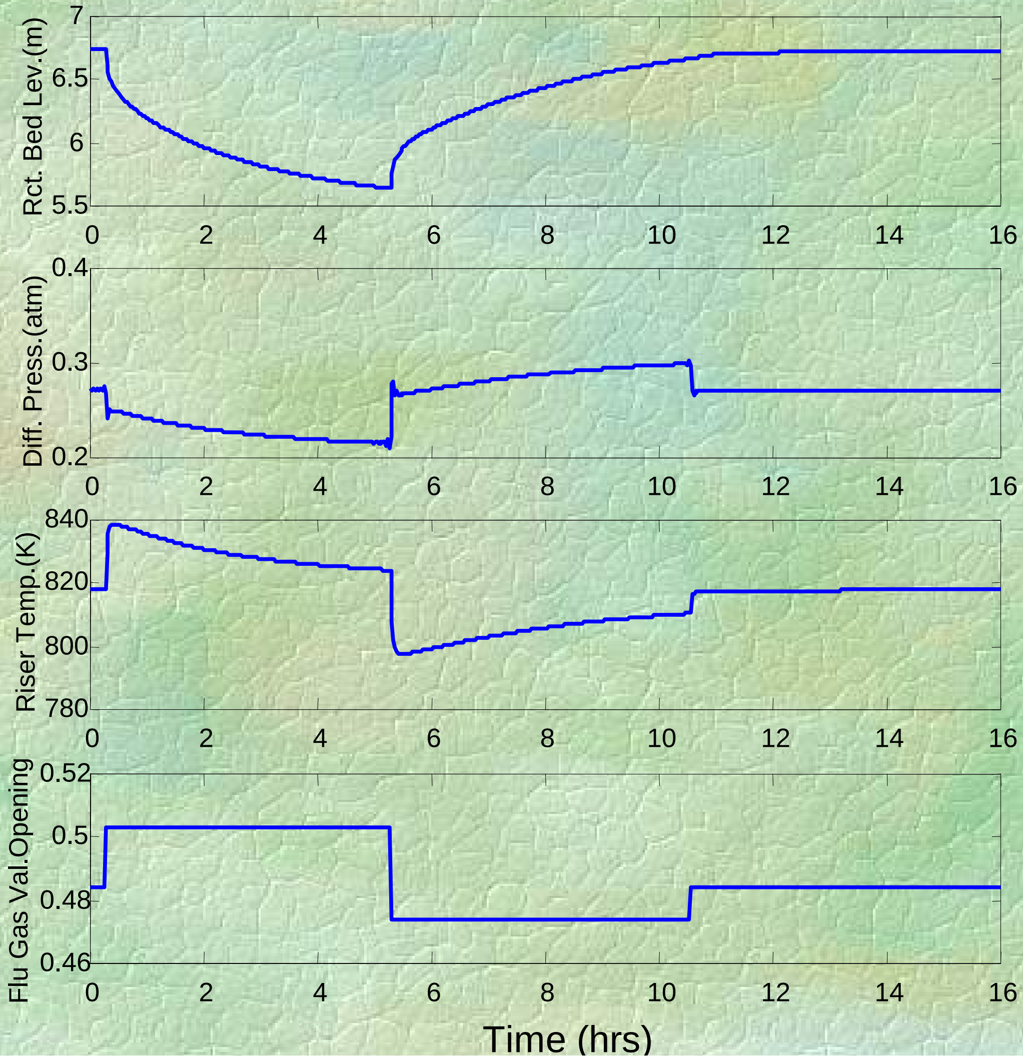

© Goodwin, Graebe, Salgado , Prentice Hall 2000

Figure 5: *Transient response of the system for input changes in the spent catalyst valve opening. (10% step increase at 0.5 hrs, 13% step decrease at 5.2 hrs, 3% increase at 10.5 hrs).*

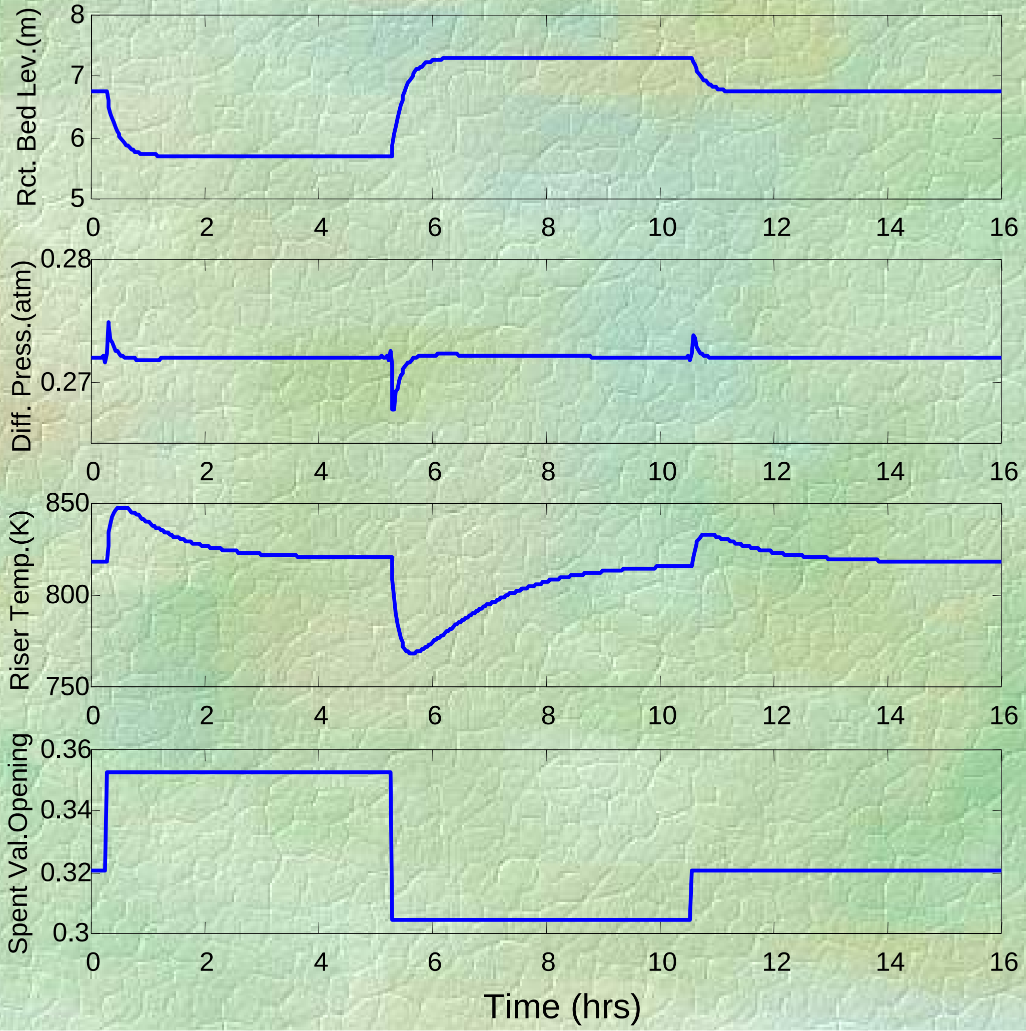

© Goodwin, Graebe, Salgado , Prentice Hall 2000

Closed loop control simulation with PI controllers

The controller parameters are fine tuned and still so fragile that the process can be easily out of control. Responses are shown in Figures 6-8.

Figure 6: *Closed loop response of the system with PI controller for a 5^{o}C step increase in the riser temperature setpoint, followed by a 10^{o}C step decrease.*

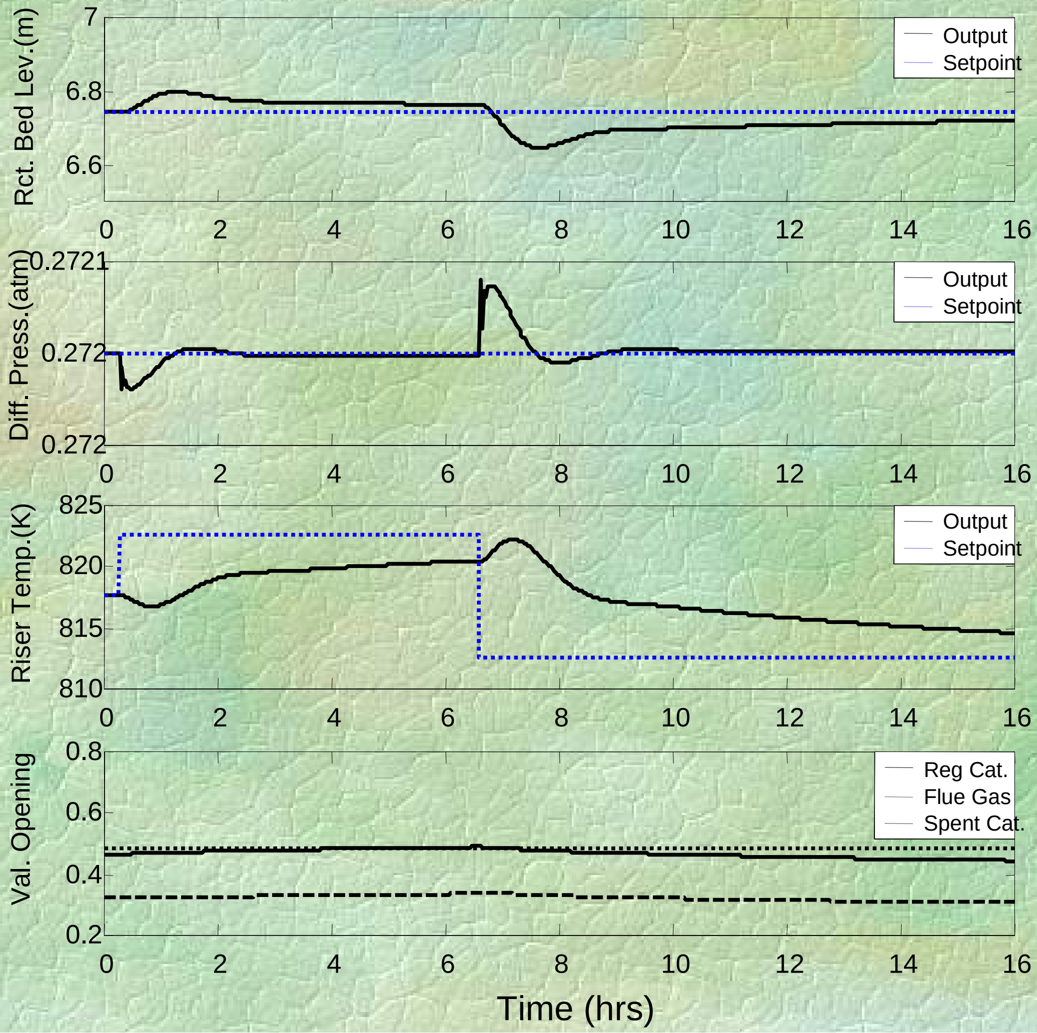

© Goodwin, Graebe, Salgado , Prentice Hall 2000

Figure 7: *Closed loop response of the system with PI controller for a 0.03atm step increase in the differential pressure setpoint, followed by a 0.05atm step decrease.*

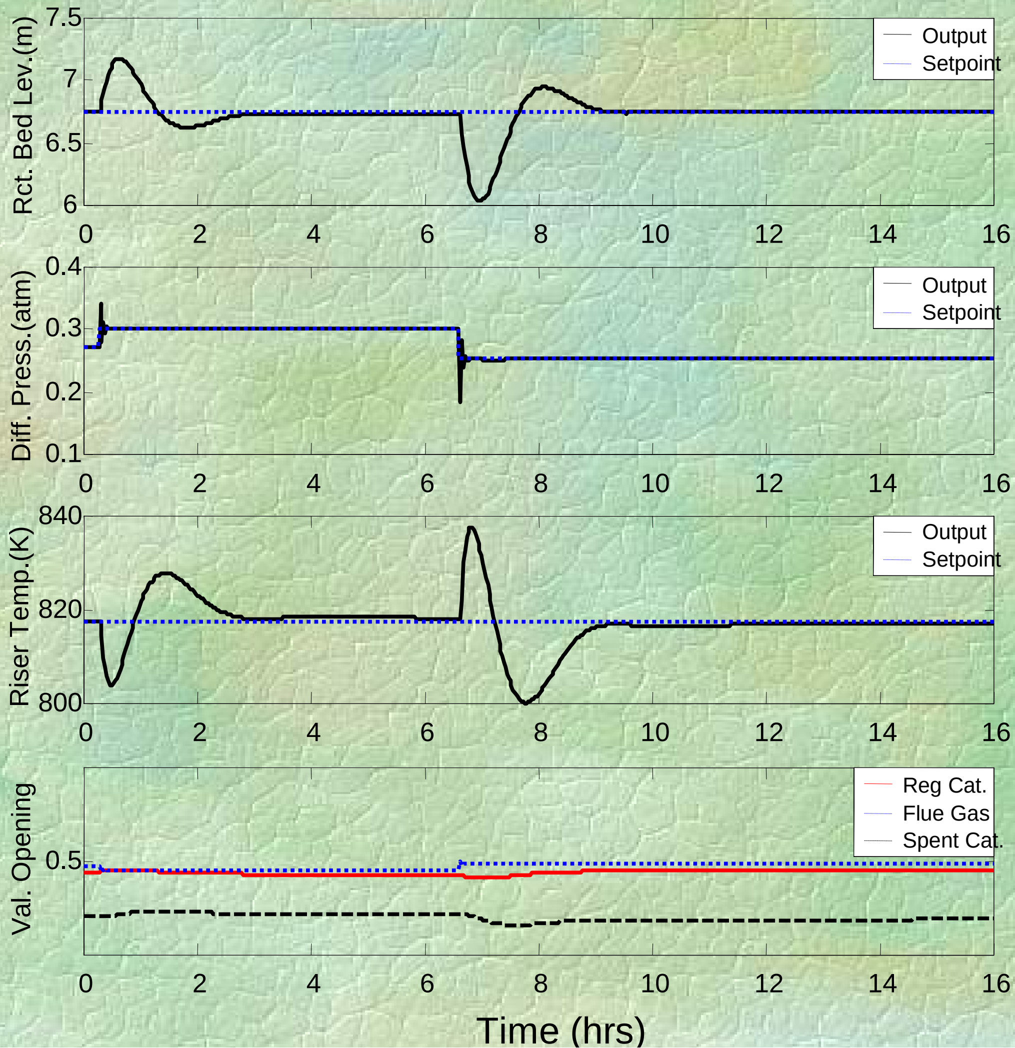

© Goodwin, Graebe, Salgado , Prentice Hall 2000

Figure 8: *Closed loop response of the system with PI controller for a 0.7m step increase in the reactor bed level setpoint, followed by a 1.2m step decrease.*

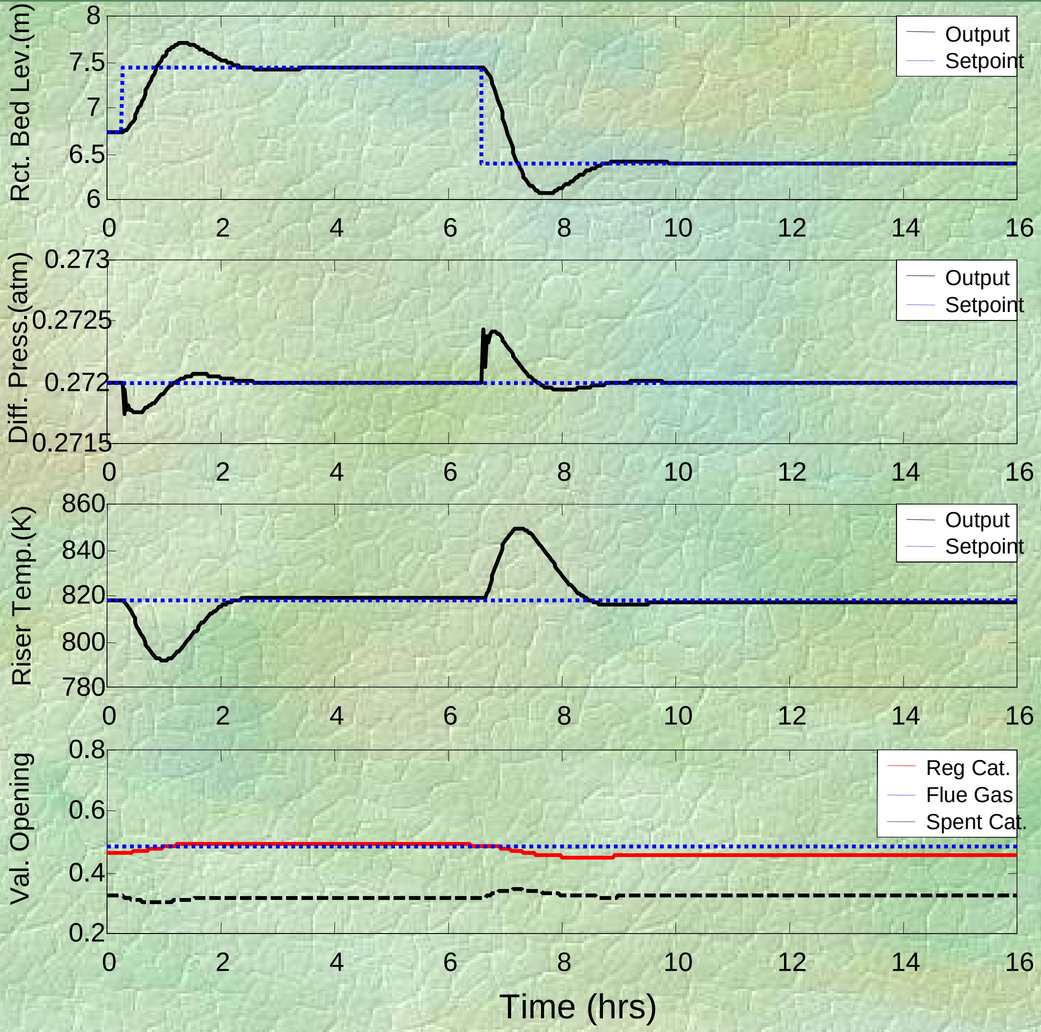

MPC Closed loop simulation

Process sampling interval:	$delt = 1$,
Output weights:	$ywt = [1 \quad 1 \quad 1]$,
Input weights:	$uwt = [0 \quad 0 \quad 0]$,
Prediction horizon (steps):	$p = 60$,
Manipulated variable moves:	$m = 60$,
Input constraints:	$u_i = [0 \;\; 100\%]; \Delta u_i = 0.1\%$
	$I = 1,2,3$

The simulink block diagram is shown as Figure 9.

The MPC control results both in setpoint change and disturbance rejection are shown in Figures 10~15.

© Goodwin, Graebe, Salgado , Prentice Hall 2000

Figure 9: *System closed loop control block diagram in Simulink.*

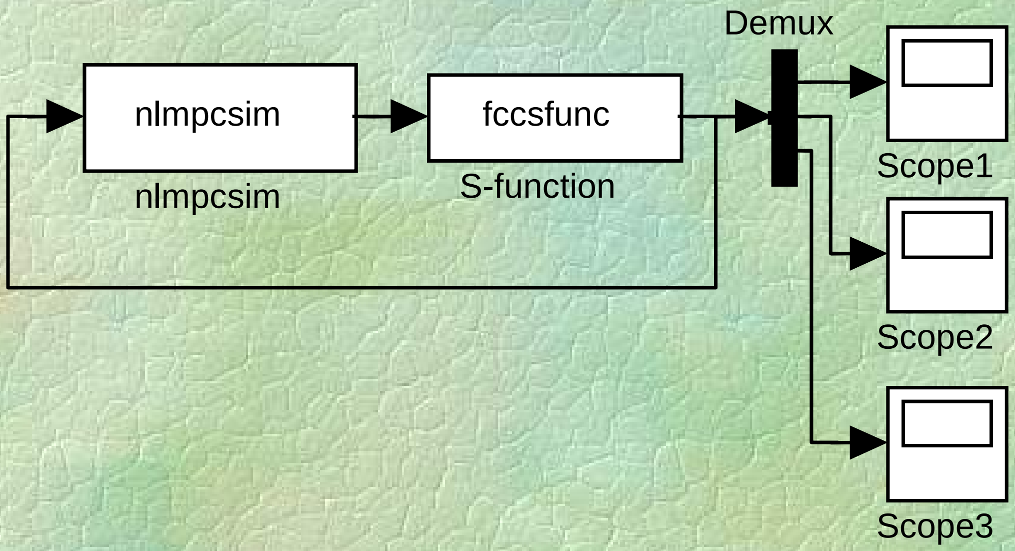

© Goodwin, Graebe, Salgado , Prentice Hall 2000

Figure 10: *Closed loop response of the system with MPC controller for a 22^{o}C step increase in the riser temperature setpoint at 5min, followed by a 50^{o}C step decrease at 30min, then a 28^{o}C step increase at 60min.*

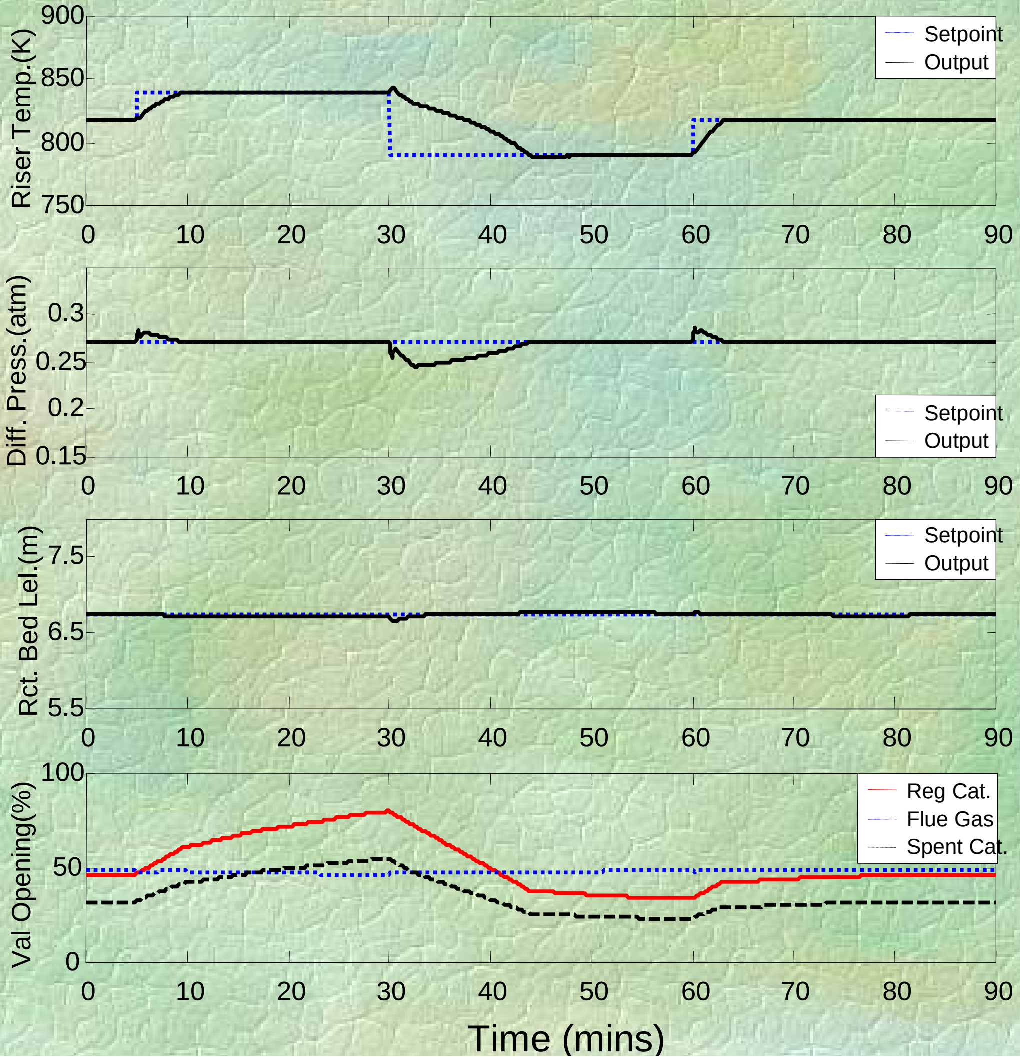

© Goodwin, Graebe, Salgado , Prentice Hall 2000

Figure 11: *Closed loop response of the system with MPC controller for a 0.08atm step increase in the differential pressure setpoint at 5min, followed by a 0.15atm step decrease at 30min, then a 0.07atm step increase at 60min.*

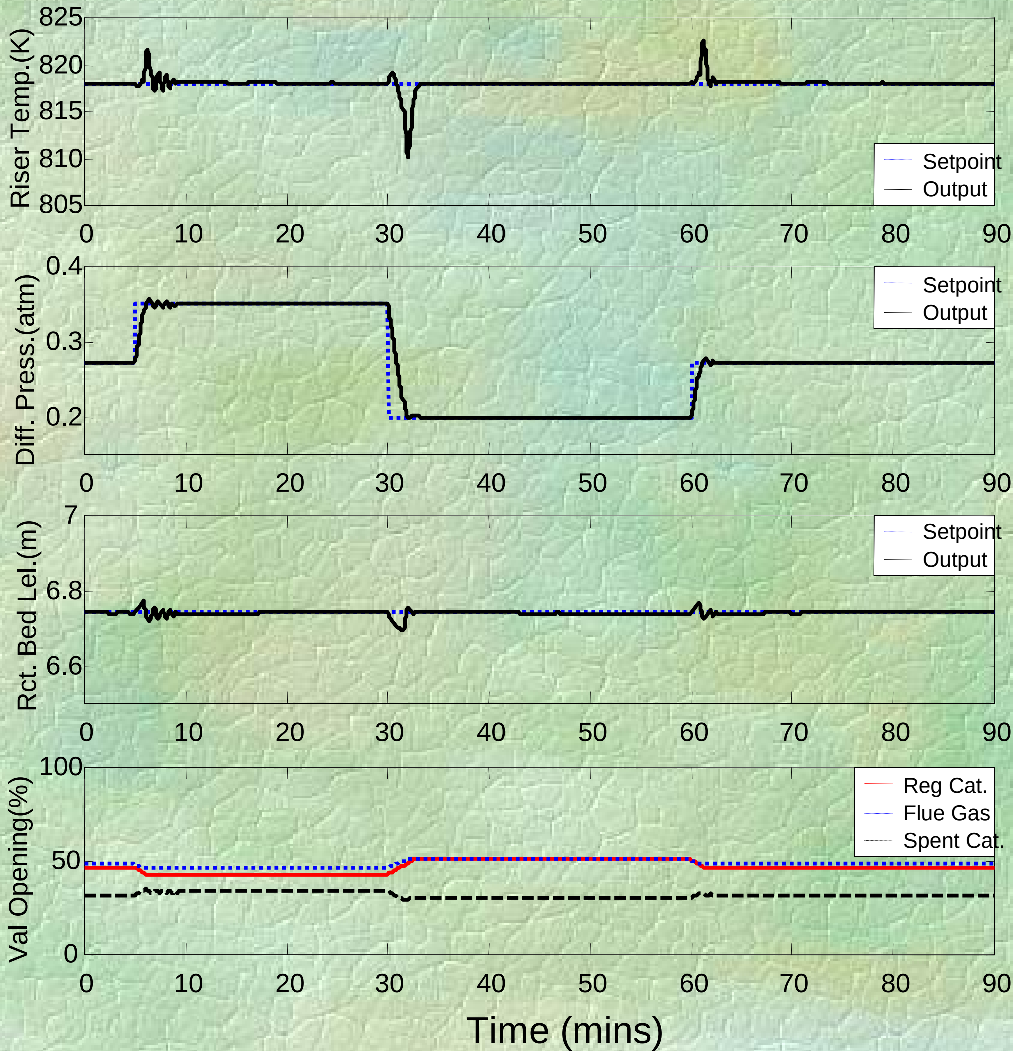

© Goodwin, Graebe, Salgado , Prentice Hall 2000

Figure 12: *Closed loop response of the system with MPC controller for a 0.76m step increase in the reactor bed level setpoint at 5min, followed by a 1.5m step decrease at 30min, then a 0.74m step increase at 60min.*

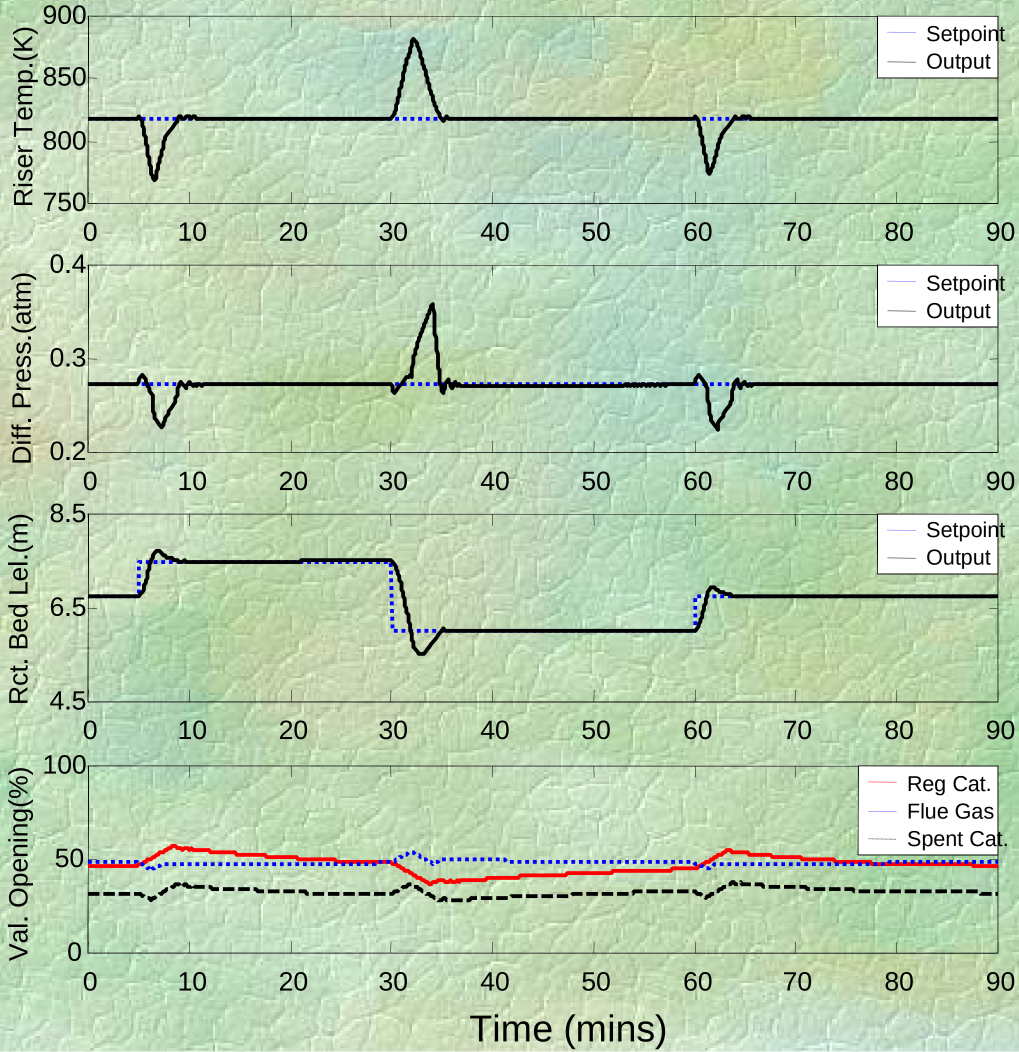

© Goodwin, Graebe, Salgado , Prentice Hall 2000

Figure13: *Closed loop response of the system with MPC controller for step changes in the riser outlet temperature, differential pressure and reactor bed level setpoints simultaneously.*

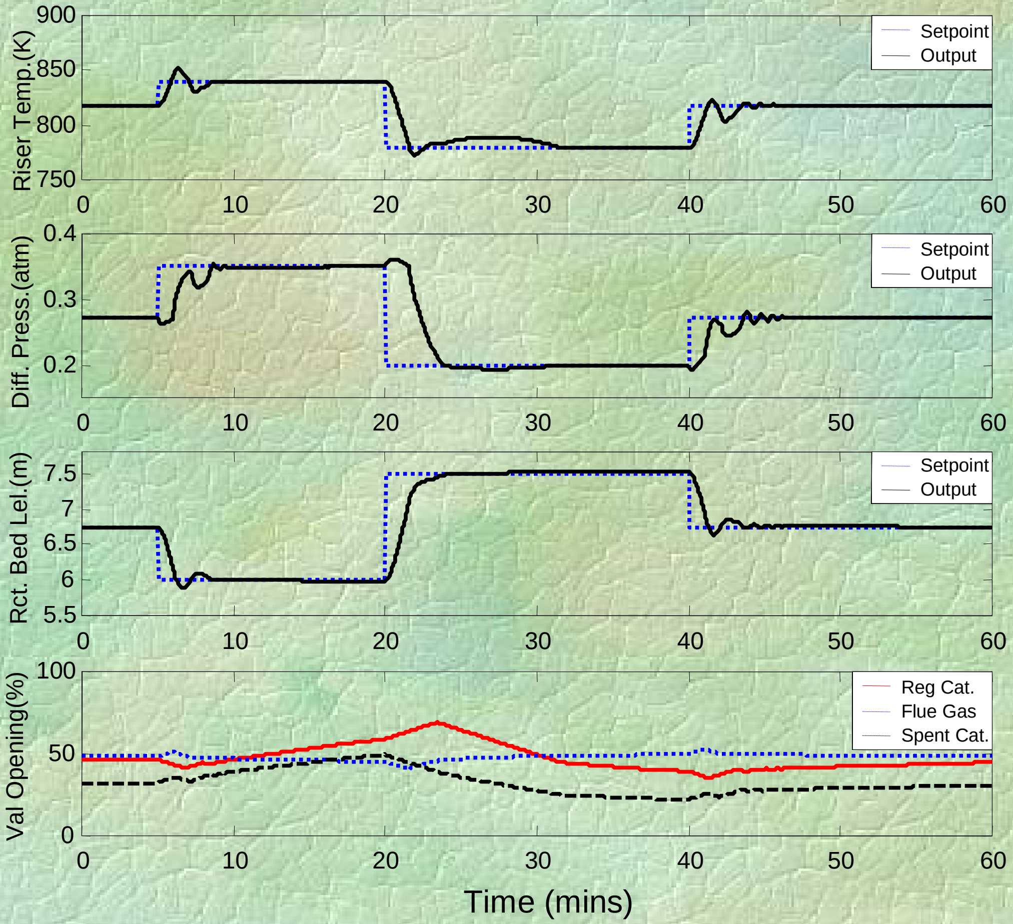

(1) 22°C step increase in riser outlet temperature setpoint, 0.08atm step increase in differential pressure setpoint, 0.74m step decrease in reactor bed level setpoint at 5min.

(2) 50°C step decrease in riser outlet temperature setpoint, 0.15atm step decrease in differential pressure setpoint, 1.5m step increase in reactor bed level setpoint at 20min.

(3) 28°C step increase in riser outlet temperature setpoint, 0.07atm step increase in differential pressure setpoint, 0.76m step decrease in reactor bed level setpoint at 40min.

© Goodwin, Graebe, Salgado , Prentice Hall 2000

Figure 14: *Closed loop response of the system with MPC controller for step changes in the riser outlet temperature, differential pressure and reactor bed level setpoints simultaneously.*

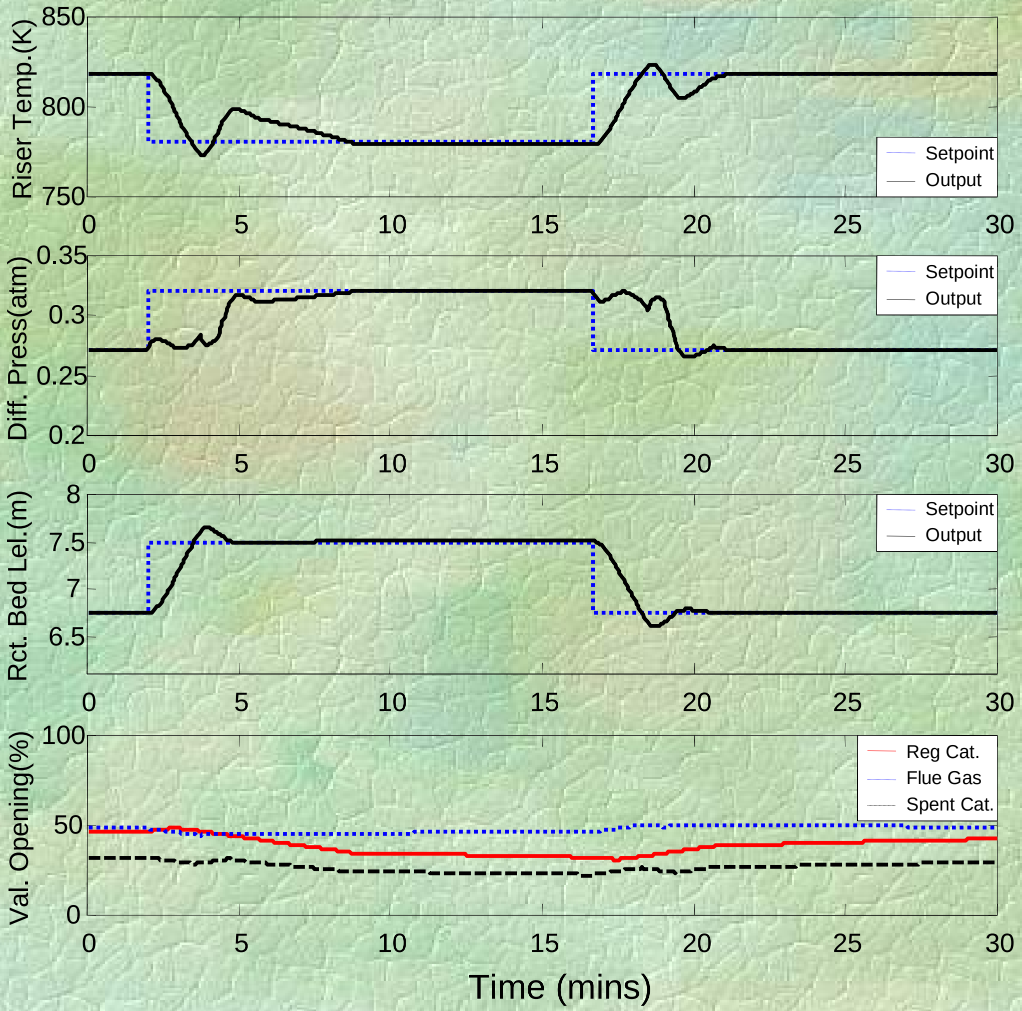

(1) 28^{o}C step decrease in riser outlet temperature setpoint, 0.08atm step increase in differential pressure setpoint, 0.76m step increase in reactor bed level setpoint at 2min.

(2) 28^{o}C step increase in riser outlet temperature setpoint, 0.08atm step decrease in differential pressure setpoint, 0.76m step decrease in reactor bed level setpoint at 17min.

© Goodwin, Graebe, Salgado , Prentice Hall 2000

Figure 15: *Closed loop response of the system with MPC controller for a 20% increase in the feed gas flow rate and 5% increase in air flow rate as disturbances at 2min, followed by 40% and 10% decrease at 15min, 40% increase in the feed gas flow rate at 30min, 40% decrease in the feed gas flow rate and 10% increase in air flow rate at 45min, 20% increase in the feed gas flow rate and 5% decrease in air flow rate at 60min.*

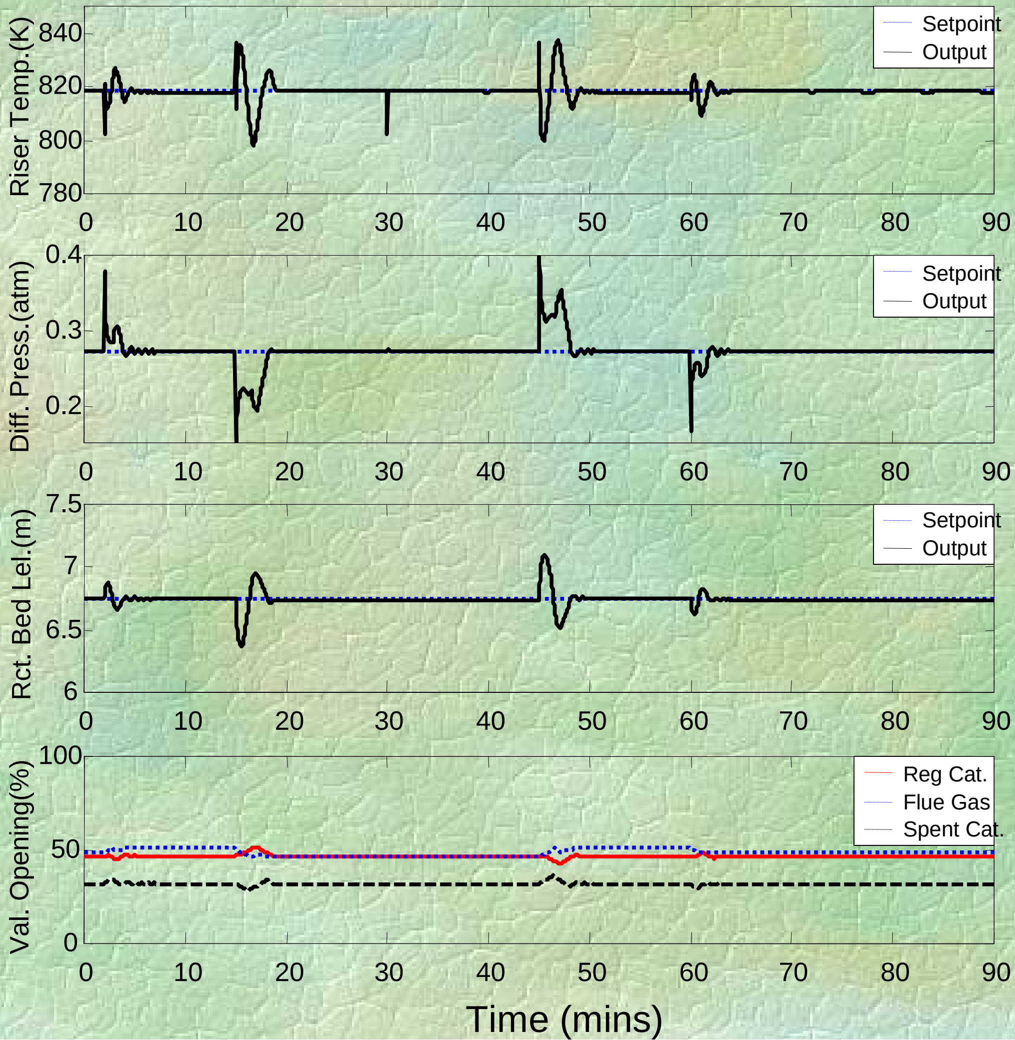

© Goodwin, Graebe, Salgado , Prentice Hall 2000

Conclusion

- MPC control strategy is far more powerful than traditional PI controller in FCC unit, with multivariable, strong nonlinearity, severe coupling, strict operating constraints.
- Make the operation smooth and stable, reducing much impact on the process and therefore much off-spec products.
- The identified model is accurate enough for MPC control purpose.
- Based on the success of the MPC simulation on FCC model, we are confident that the following objectives will be achieved in an industrial practice:

© Goodwin, Graebe, Salgado , Prentice Hall 2000

- Improving the process operating stability .
- Maximizing the process throughput and desirable products yield.
- Improving the product quality.
- Minimizing energy consumption.
- Improving unit’s economic performance.

© Goodwin, Graebe, Salgado , Prentice Hall 2000

Summary

- MPC provides a systematic procedure for dealing with constraints (both input and state) in MIMO control problems.
- It has been widely used in industry.
- Remarkable properties of the method can be established, e.g. global asymptotic stability provided certain conditions are satisfied (e.g. appropriate weighting on the final state).

© Goodwin, Graebe, Salgado , Prentice Hall 2000

- The key elements of MPC for linear systems are:
  - state space (or equivalent) model,
  - on-line state estimation (including disturbances),
  - prediction of future states (including disturbances),
  - on-line optimization of future trajectory subject to constraints using Quadratic Programming, and
  - implementation of first step of control sequence.

Embellishments

The results presented in this chapter suggest there is a close connection between MPC and anti-windup provided the demands made on the system are not too severe.

Actually, recent research has shown that there exists a non-trivial region of state space in which MPC and anti-windup are equivalent.

The next slides illustrate this idea.

© Goodwin, Graebe, Salgado , Prentice Hall 2000

Illustrative Example

$$A=\begin{bmatrix}1 & 0\\ 0.4 & 1\end{bmatrix}, B=\begin{bmatrix}0.4\\ 0.08\end{bmatrix}, C=\begin{bmatrix}0 & 1\end{bmatrix},$$

This is the zero-order hold discretisation (with sampling period T_s - 0.4 sec.) of the double integrator

$$\begin{aligned}\dot{x}_1(t)&=u(t),\\ \dot{x}_2(t)&=x_1(t),\\ y(t)&=x_2(t).\end{aligned}$$

- Saturation level: $\overline{U}=1$
- Fixed horizon: $N=10$

© Goodwin, Graebe, Salgado , Prentice Hall 2000

Regions of State Space: A : *Region where no saturation occurs*

B : *Region in which MPC and anti-windup are equivalent.*

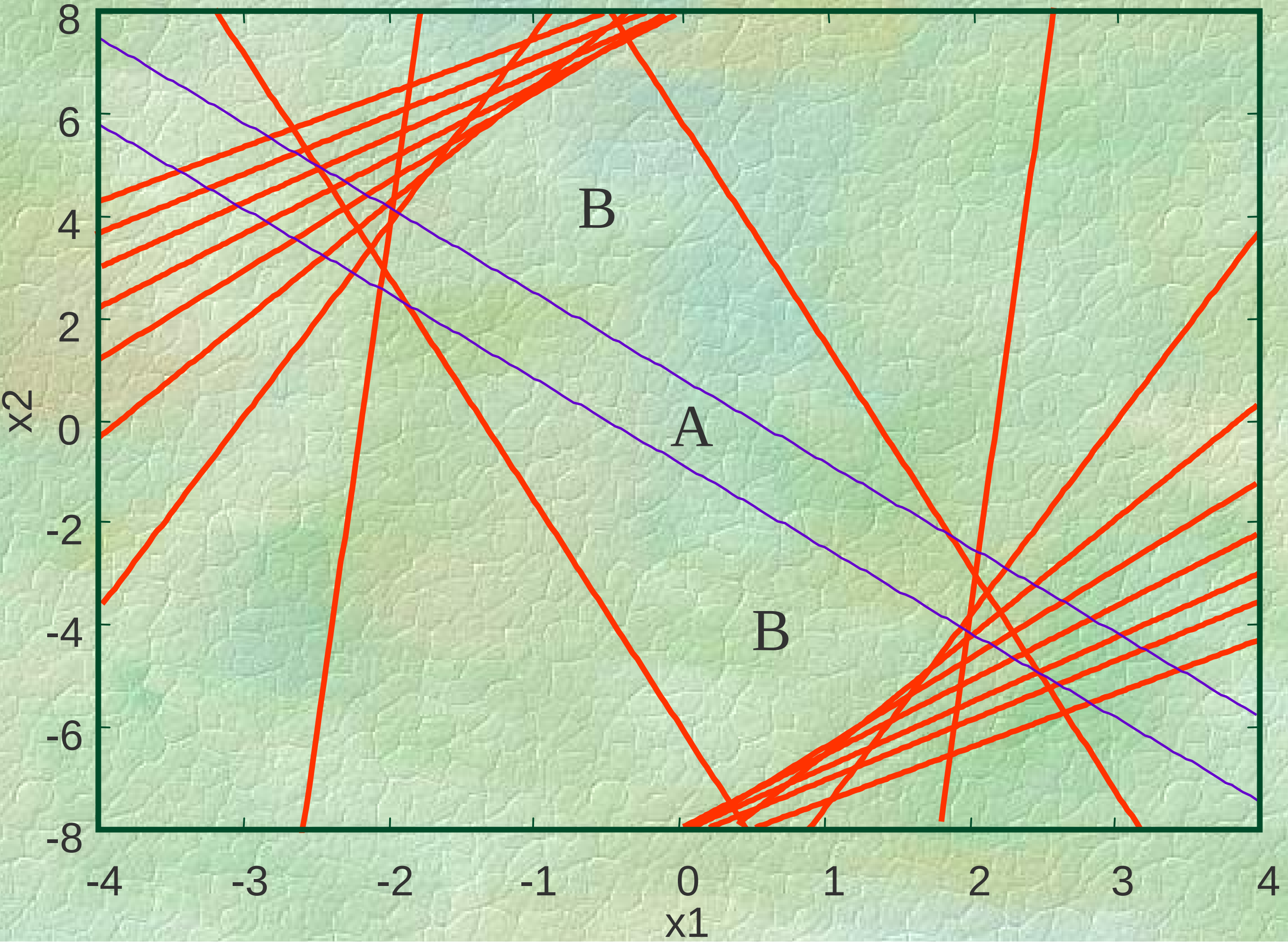

© Goodwin, Graebe, Salgado , Prentice Hall 2000

First Step of MPC starting from a point in state space in which MPC ≡ anti-windup but where input saturation occurs

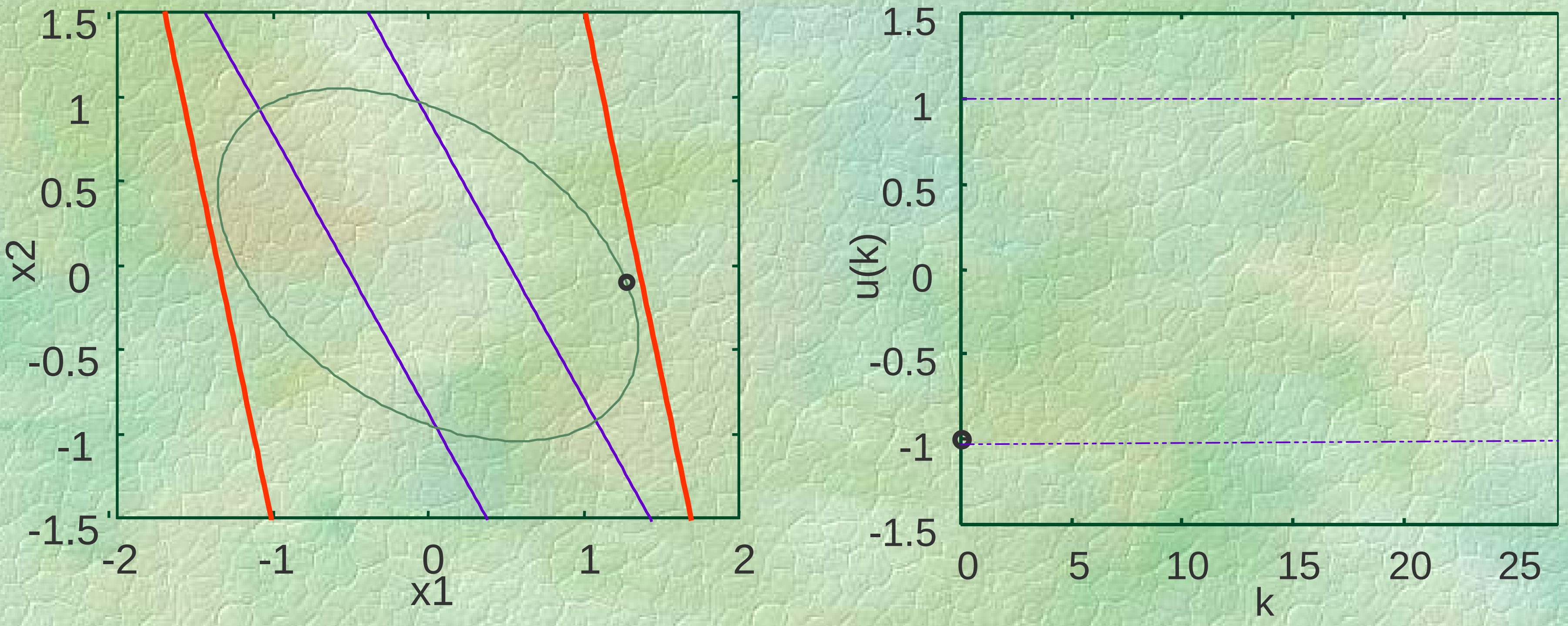

Second Step - *Note input still saturated*

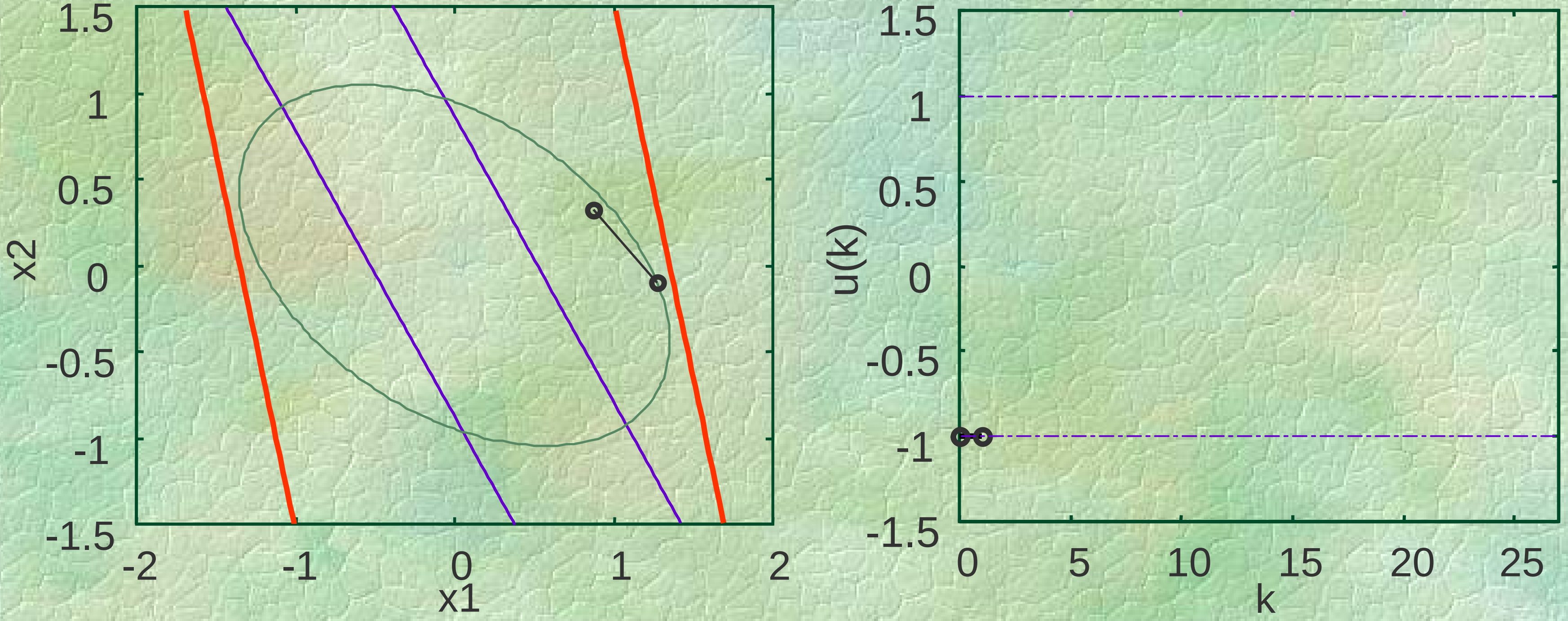

© Goodwin, Graebe, Salgado , Prentice Hall 2000

Third Step - *Note input still saturated*

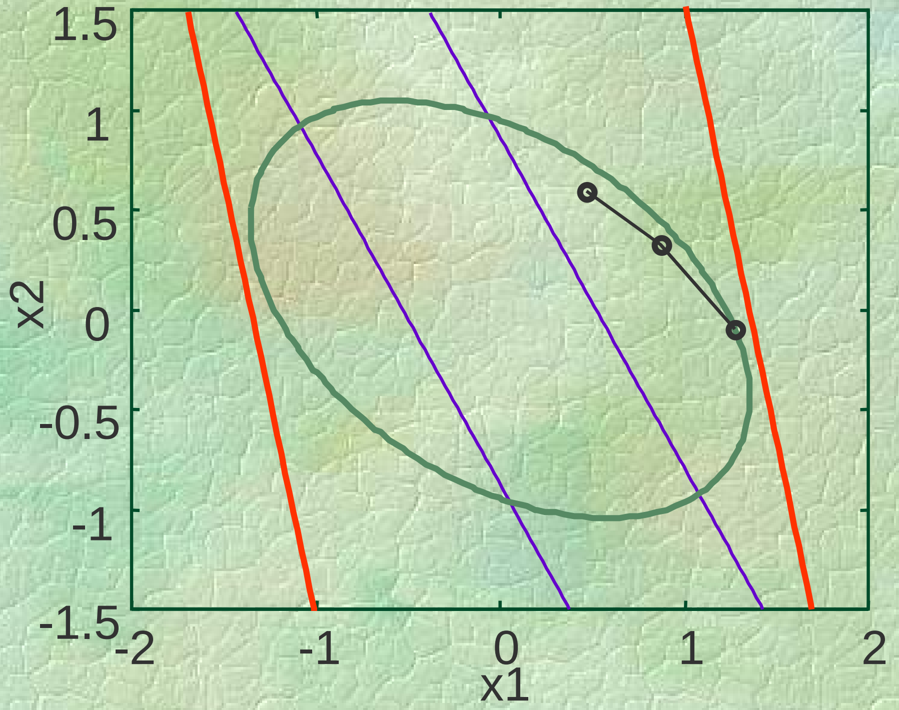

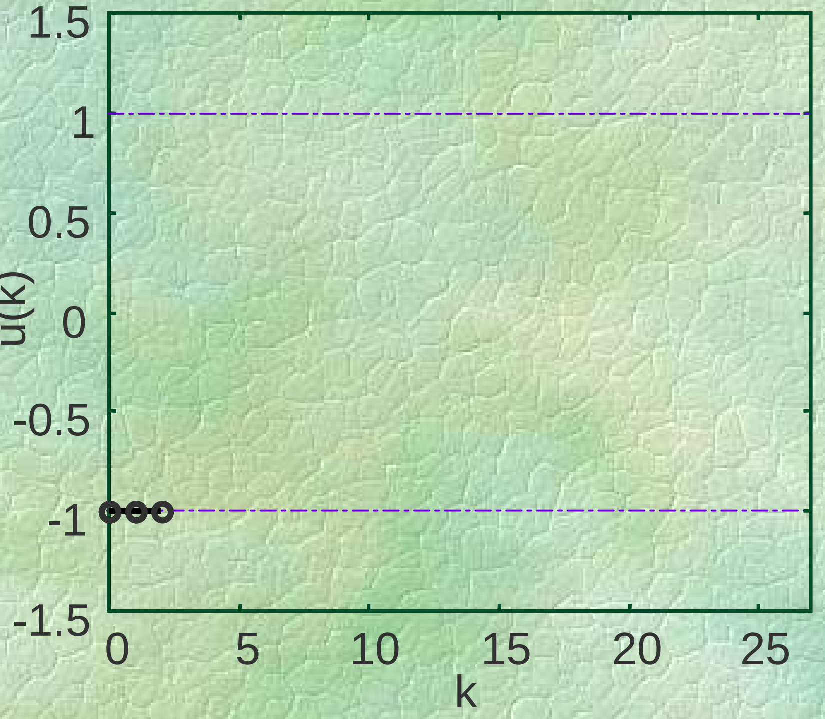

© Goodwin, Graebe, Salgado , Prentice Hall 2000

Fourth Step - *Note that state has entered region in which input is no longer saturated*

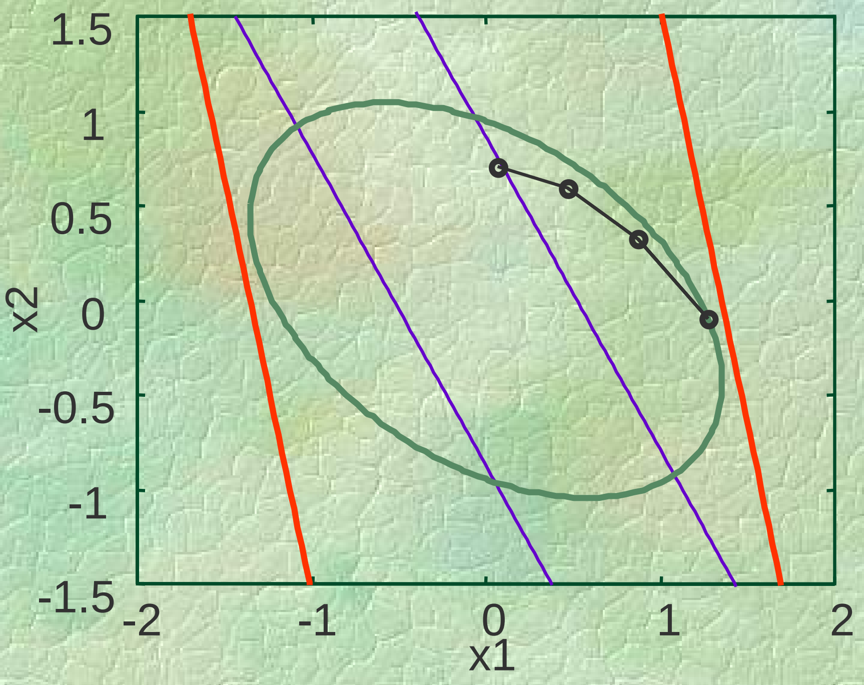

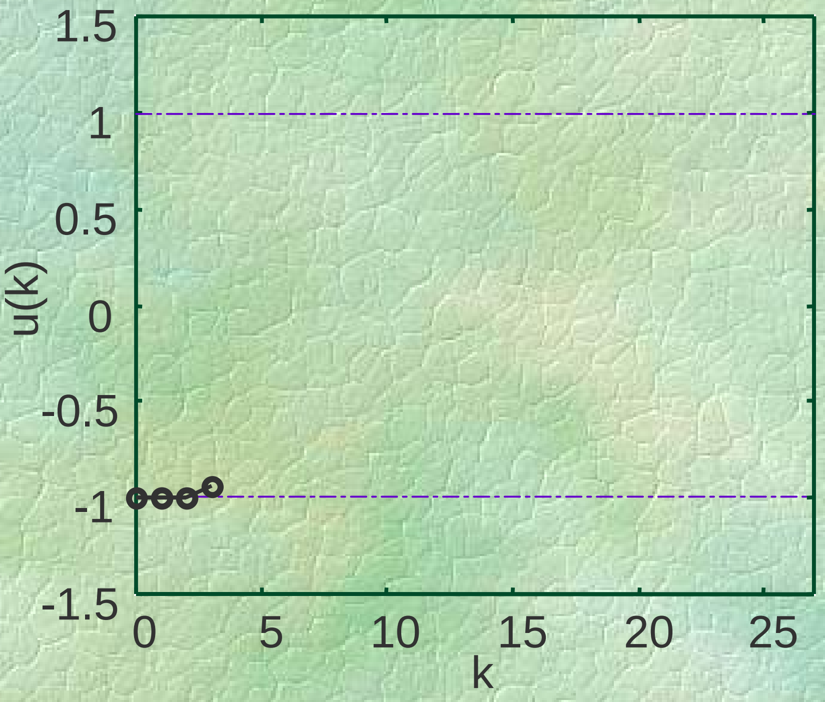

© Goodwin, Graebe, Salgado , Prentice Hall 2000

Remainder of the response - *Note input remains unsaturated*

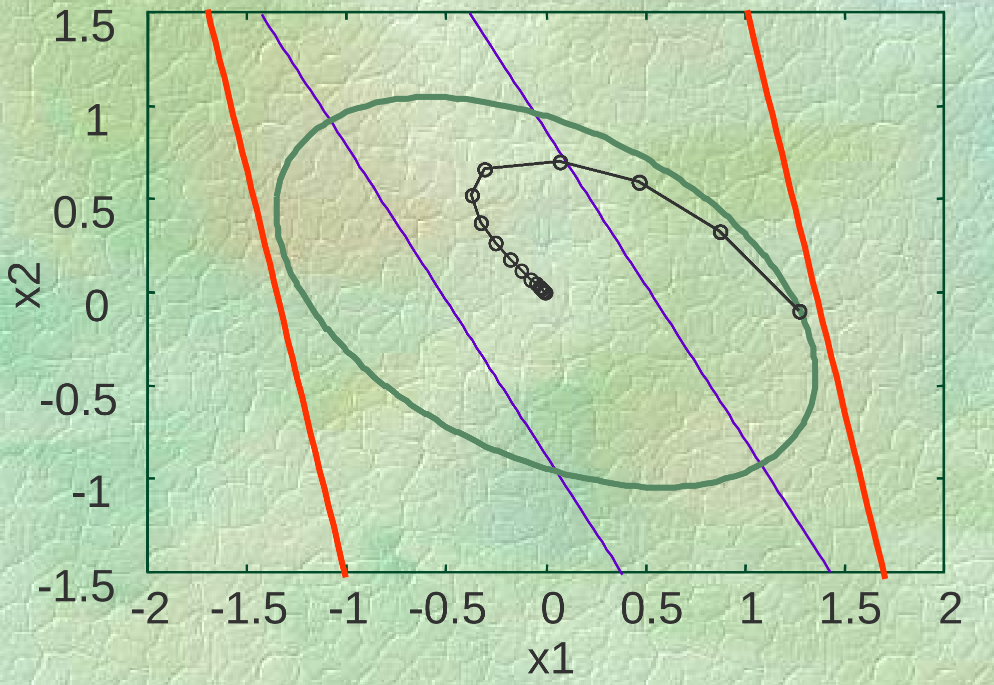

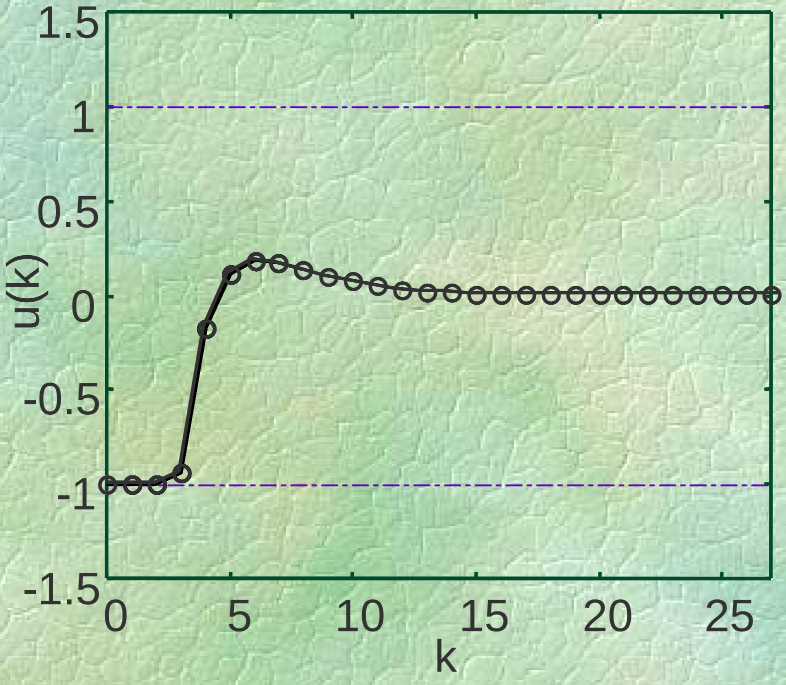

Overlay the anti-windup Solution - *Note that MPC and anti-windup give the same solution for this particular initial condition*

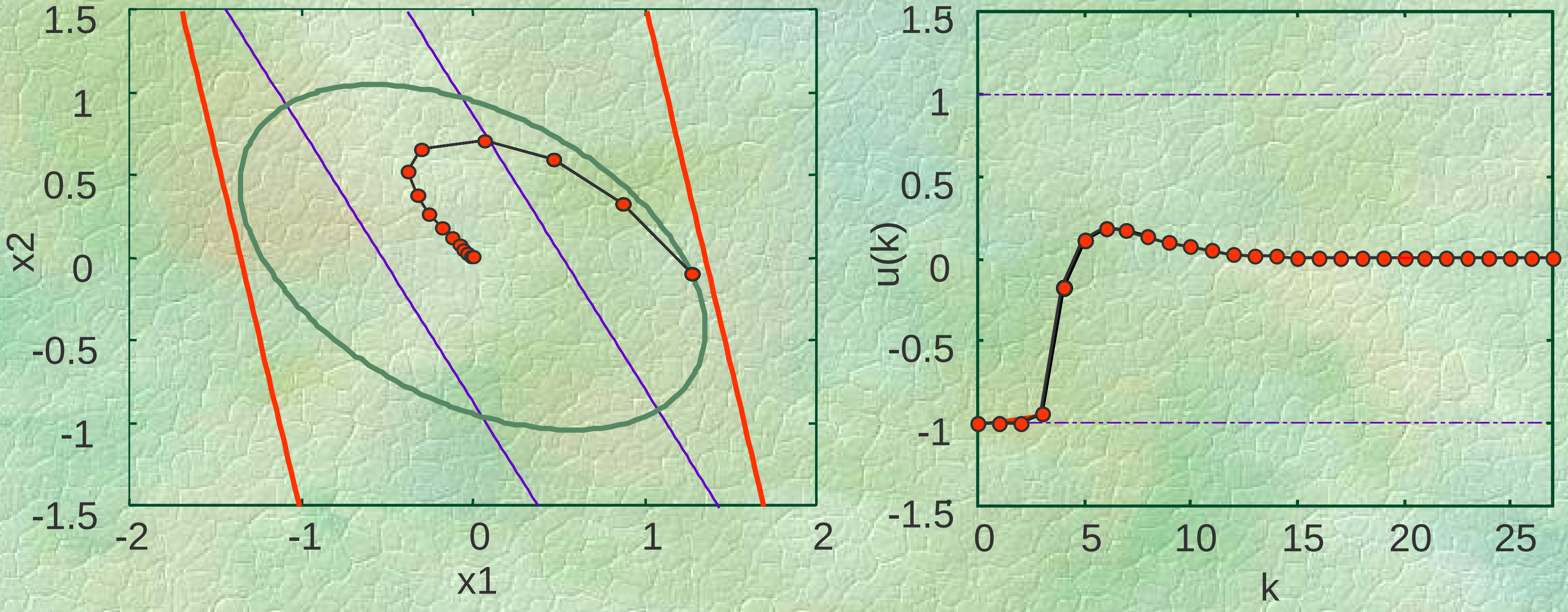

© Goodwin, Graebe, Salgado , Prentice Hall 2000

Observations

1. It is not surprising that anti-windup performs well in some cases because it can be shown that there is a non-trivial region of state space in which anti-windup and MPC are equivalent.
2. However, caution is needed in interpreting this result. In general, anti-windup is too shortsighted and MPC will perform better.
3. Some of these issues are explored in the problems for readers given in the book.